Experimental Study and Optimization of the Machining Parameters in Ultrasonic Vibration-assisted Turning (UVT)

A THESIS SUBMITTED IN PARTIAL FULFILLMENT
OF THE REQUIREMENTS FOR THE DEGREE OF

MASTER OF TECHNOLOGY
IN
MECHANICAL ENGINEERING

BY

VIVEKANANDA KUKKALA
210ME2134

UNDER THE GUIDANCE OF

Prof. S.K. SAHOO

DEPARTMENT OF MECHANICAL ENGINEERING
NATIONAL INSTITUTE OF TECHNOLOGY
ROURKELA
2012

National Institute of Technology

Rourkela

CERTIFICATE

This is to certify that the thesis entitled, **"Experimental Study and Optimization of the Machining Parameters in Ultrasonic Vibration-assisted Turning (UVT)"** submitted by Mr. VIVEKANANDA KUKKALA in partial fulfillment of the requirements for the award of *Master of Technology* degree in *Mechanical Engineering* with specialization in *Production Engineering* during session 2010-2012 at the National Institute of Technology, Rourkela (Deemed University) is an authentic work carried out by him under my supervision and guidance. To the best of my knowledge, the matter embodied in the thesis has not submitted to any other University/Institute for the award of any degree or diploma.

Date:

Place:

Prof. S.K. Sahoo
Dept. of Mechanical Engg.
National Institute of Technology

ACKNOWLEDGEMENT

I express my deep sense of gratitude and reverence to my thesis supervisor **Prof. S. K. Sahoo**, Professor, Mechanical Engineering Department, National Institute of Technology, Rourkela, for his invaluable encouragement, helpful suggestions and supervision throughout the course of this work and providing valuable department facilities.

I would like to thank **Prof. K. P. Maity**, Head of the Department, **Prof. S. S. Mahapatra,** PG coordinator of the Mechanical Engineering Department and **Prof. S. K. PATEL**, faculty Adviser.

I would like to thank **Mr. Kunala Nayak** Production lab technician, **Mr. Elias Eliot** (Mtech (R)), **Mr. kalinga Bal** (Mtech), **Mr. Kumar Abhishek** (Mtech), **Mr. Anshuman Kumar** (M.tech) and **Mr. S.K.Sahu** (P.hd scholar) for their timely help in conducting the experiment.

Last but not least I would like to thank **my parents** and well-wishers who are involved directly or indirectly in successful completion of the present work.

Date **(Vivekananda Kukkala)**

210ME2134

ABSTRACT

In recent year's applications of hard materials in different industries, like aviation, defense and petrochemicals sectors etc. have been increased remarkably. The machining of these hard materials is very difficult in conventional turning process. Ultrasonic assisted turning is a suitable and advanced process for machining hard and brittle material because of its periodic cutting mechanism. In the present work, an ultrasonic vibratory tool (UVT) is designed and analyzed using ANSYS® environment for calculation of its natural frequency and working amplitude of vibration. An ultrasonic assisted turning system is designed in consideration of cutting tool as a cantilever beam. Experimental study has been carried out to find the difference between ultrasonic-assisted turning and conventional turning at different cutting conditions taking Stainless steel (a general purpose engineering material) as the work piece material. It is found that ultrasonic assisted turning reduces the surface roughness and cutting forces in comparison with conventional turning. It is well known that cutting forces and surface finish/roughness are two major parameters which affect the productivity of the turning process. In the present work, Taguchi with TOPSIS method is used to optimize both forces and surface roughness to find the best possible machining parameters under the used experimental working conditions.

Key words: *UAT, UVT, Longitudinal vibration, Modal analysis, Harmonic analysis, Triangular rule, GRA, RSM*

ABBREVIATIONS

TOPSIS	Technique for Order Preference by Similarity to Ideal Solution
ANOVA	Analysis of variance
ANSYS	Analysis of system
CNC	Computer numerical control
CT	Conventional turning
1D	One-dimensional
2D	Two-dimensional
3D	Three dimensional
DAQ	Data acquisitions
DOE	Design of experiment
DOF	Degree of freedom
FEM	Finite element modeling
FRF	Frequency response function
Hz	Hertz
MB	Mega byte
MS	Mean square
NC	Numerical control
PC	Personal computer
PZT	Piezoelectric transducer
RAM	Random access memory
SEM	Scanning electron microscope
SS	Sum of square
TWCR	Tool work-piece contact ratio
UAC	Ultrasonic assisted cutting
UAT	Ultrasonic assisted turning
UVT	Ultrasonic vibratory tool

NOMENCLATURE

A	Area of cross section
A	Amplitude
A_c	Acceleration
C	Velocity of sound
Cos	Cosine
D	Diameter
D	Depth of cut
E	Young’s modulus
F_m	Forces of momentum
F_x	Cutting force in X-axis direction
F_y	Cutting force in Y-axis direction
F_z	Cutting force in Z-axis direction
f	Frequency
h	Height
I	Complex number
K	Stress concentration
L	Length
M	Mass
M_z	Moment in Z-axis direction
N	Spindle speed
R_a	Surface roughness
R	Radius
S	Feed
Sin	Sine
S	Stress
S_m	Maximum stress
T	Time
V	Cutting velocity

V_c	Velocity of chip
V_t	Velocity of tip
V	Velocity
W	Weight
X_n	Nodal plane
Λ	Wave length
Γ	Poison's ratio
ξ	Displacement
ξ_M	Maximum displacement
ρ	Density
ω	Angular velocity

CONTENTS

List of Figures

List of Tables

Chapter 1

1. INTRODUCTION

1.1 Introduction of UAT

Ultrasonic vibration has been harnessed with considerable benefits for a variety of manufacturing processes, for example, ultrasonic cleaning, plastic welding, etc. In typical ultrasonic machining, high frequency electrical energy is converted into mechanical vibrations using a transducer or booster combination, which are transmitted through a horn or tool assembly. Ultrasonic assisted turning is a cutting technique in which a certain frequency (in ultrasonic range) of vibration is applied to the cutting tool or the work-piece (besides the original relative motion between these two) to achieve better cutting performance (Shamoto et al. [1]). A number of experimental setup has been proposed to make the process simpler, but the tendency is to apply the process to a wide range of materials and to study the effect of machining parameters. Many researchers have reported significant improvements in noise reduction, tool wear reduction, surface finish, etc. by applying ultrasonic vibration during machining operations in general, the turning processes in particular [2, 3]. This pointed out possible advantages of the ultrasonic technology for industrial machining. The present research is particularly focused on ultrasonic vibration-assisted turning.

In ultrasonic assisted machining, vibration amplitude (normally sine wave) lead to an alternating gap during cutting and was identified as an important mechanism in vibration cutting. Increasing the vibration amplitude means an enlargement in the gap that allows more cutting fluid to extract the heat during the cutting process, thus enhancing the tool's life, improved work-piece finish, reduction in cutting forces and decreasing the chance of build-up-edge formation [4-5]. In turning process there are three independent principal directions in which ultrasonic vibration can be applied (Figure 1.1).Significant advantages were obtained when the usual continuous interaction between the cutting tip and the work-piece was replaced by intermittent cutting [6-7]. However, when the cutting tip is vibrated ultrasonically the following restrictions are imposed:

$$\text{Tangential direction: } V_c=\pi ND < V_t=2\pi a f \quad (1)$$

Where V*c* is the cutting speed during turning operation, N is the rotational speed of work-piece, Vt is the tip velocity, *f* is the frequency of vibration and *a* is the amplitude of vibration. A rheological model of ultrasonic vibration cutting projected by Astashev [8] and ensuing experiments confirmed a evident reduction in the cutting force for ultrasonic cutting with vibration in tangential direction (f =20kHz, a=10μm). It was also reported that cutting force reduction was less at higher cutting speeds and, with a cutting speeds exceeding a certain level ($V_t > \omega$, where ω is the angular frequency), vibration did not affect the cutting force. The resistance forces were considered to be caused by plastic deformation of the layer being cut off by frictional forces acting on the working faces of the cutting tool. These experimental results have been explained theoretically by Astashev and Babitsky [9] within the frame work of rheological models. Reduction in the cutting force caused by superimposition of ultrasonic vibration was derived for the elasto-plastic material model. It was concluded that the vibrating process transforms and reduces the friction force due to the effect of dynamic fluidization of dry friction. Dynamic characteristics of transformed machining processes were obtained, including the dependence of reduced cutting forces on the material and vibrations parameters. Dynamics of an ultrasonic cutting machine under technological load was investigated and the nonlinear amplitude response of vibrating tool in the process of cutting was obtained by many researchers.

The auto resonant control system keeping the resonant conditions of excitation under variable technological loads was constructed by Astashev and Babitsky [9].

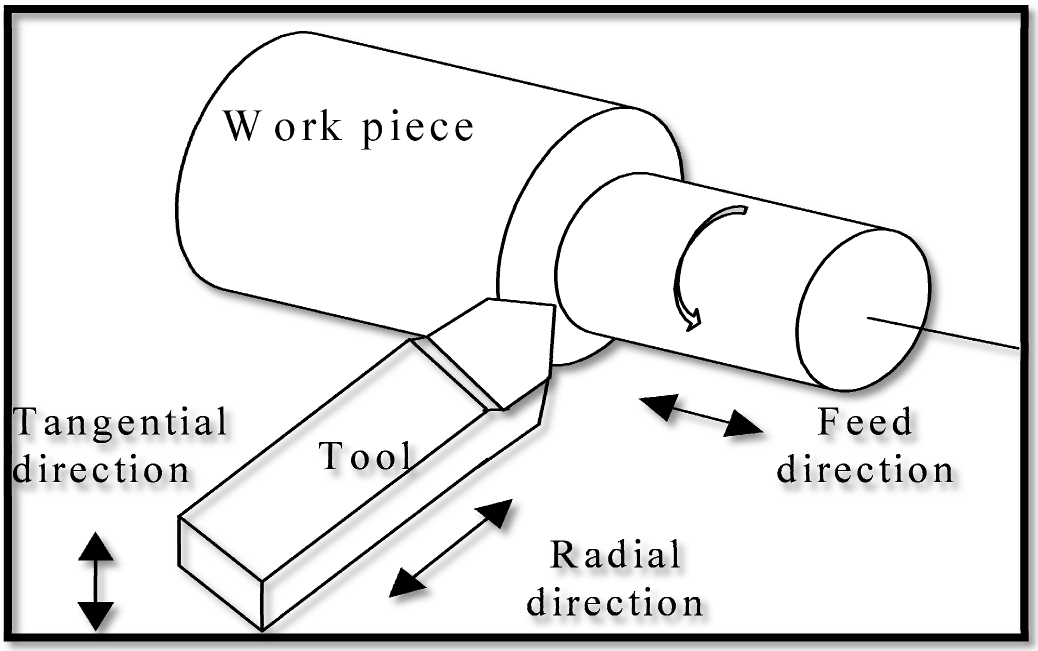

Figure1. Principal vibration directions during ultrasonically assisted turning.

Babitsky et al [9] designed an auto resonant ultrasonic assisted turning system, maintaining the constant level of vibration provided by the transducer and therefore improving the precision of ultrasonic machining. Vibration in the feed directions was also studied. It was pointed out that application of ultrasonic vibration along the feed direction enables overcoming the restriction on the level of rotational speeds, which is of great importance for industrial UAT requiring high levels of productivity.

Mashiko and Murakawa [10] developed practical ultrasonic vibration cutting tool system and their investigation on tool wear and surface finish in ultrasonic and conventional turning and they found that chipping of the cutting edge can be effectively prevented and good surface finish obtained in ultrasonic assisted turning. Mashiko and Murakawa also investigate on vibration assisted turning and they found that ultrasonic assisted turning improves surface finish and reduces average cutting forces as compared to conventional turning in case of hard and brittle material.

1.2 Present Needs in Industry

Generally the machining surface quality is usually measured by the surface roughness and physical mechanical properties of the surface layer. The surface quality has a great impact on wear resistance, fatigue strength of the product and fit precision of the part. Hard and brittle material has excellent mechanical properties at low and intermediate temperature. It plays an important part in recent years in aerospace, nuclear and petroleum industries. Hard materials are very difficult to machine because of a tendency of the maximum temperature of tool face existing at the tip of tool. Micro welding at the tool tip and chip interface takes place so as to lead to the built up edge formation which effect the surface quality of material. In ultrasonic assisted turning these effects are reduced due its vibro-impact cutting.

1.3 Aim and Objectives of the Work

1.3.1 Aim of the work

The present research aims to get a technical understanding of the ultrasonic assisted turning process against the principal cutting force and surface roughness generation. The research includes the design and FEM analysis of ultrasonic vibratory tool, design and development of an ultrasonic assisted vibration turning system, taking cutting tool as a cantilever beam. Turning carbon steel work-piece material (a general purpose engineering material) using both conventional and ultrasonic assisted turning and analyzing the results. Mathematical relations between responses and factors of ultrasonic assisted turning (UAT) are developed and the ultrasonic turning process parameters are optimized.

1.3.2 Objectives of the present work

- FEM analysis of ultrasonic vibratory tool (UVT).
- Design and manufacture of the experimental set-up.
- Experimental investigations using both conventional and ultrasonic assisted turning processes taking a general purpose engineering material (stainless steel) as work-piece.
- Comparison of both conventional and ultrasonic assisted turning based on experimental data.
- Optimization of the process parameters using grey based Taguchi with TOPSIS.

Chapter 2

2. LITERATURE SURVEY

2.1 Introduction

Now a day's manufacturing industries are very much helpful in our daily life. Ultrasonic assisted turning is one of the best manufacturing processes, for example, ultrasonic cleaning, ultrasonic grinding, ultrasonic welding and ultrasonic turning, ultrasonic drilling etc. Ultrasonic assisted turning (UAT) is a new non-conventional technique, used to remove an unwanted material to produce a desired product. First attempt to employ the ultrasonic power is attempted by Russian [2, 11] as well as Japanese [3, 12] researchers.

2.2 Experimental study on ultrasonic assisted turning

Ainhoa Celaya and Aitzol Lamikiz [13] discuss the advantages and drawbacks of Ultrasonic Assisted Turning (UAT) have been investigated focusing on the effect of tool vibration on surface quality. They are done Several experiments have been performed on mild steels changing the cutting speed, feed and depth of cut, to study how the influence of the ultrasonic vibration on the surface roughness varies depending on the cutting conditions.

The cutting tests have been performed on an universal lathe. A commercial piezoelectric transducer Master sonic MSG-2000 (range of frequencies: 17.5–24 kHz) is used to generate the ultrasonic vibration. A booster attached to the transducer is used to amplify the vibration. The design of the booster has to allow the transmission and amplification of the vibration generated in the transducer while maintaining enough stiffness to be able to cut the material without a high deflection or dynamic problems. The vibration obtained has been measured with a laser vibrometer Polytec 0FV-505.

After the experiment Ainhoa Celaya and Aitzol Lamikiz [13] experimental tests show an improvement in surface roughness up to 40% in the most favorable case when the vibration is applied in the direction of cutting speed and 6% when the vibration is applied in the feed direction. Also, it has been demonstrated trough an spectral analysis that the vibration in the cutting speed direction reduces the height of the crests produced by the tool and reduces the waviness of the generated geometry.

The roughness profiles of the surfaces machined both in conventional and with vibration cutting. It can be seen that the roughness profile of the UAT test is more uniform, and for example, it does not reach ±5 μm, as it does the conventional turning test.

2.3 Review of Ultrasonic Assisted Cutting

Ultrasonic assisted cutting technique is becoming very challenging in many recent engineering developments, especially in relation to surface finish and tool wear and material removal rate. The very basic component of ultrasonic assisted cutting system is piezoelectric transducer and ultrasonic vibratory tool. For different applications different designs have been developed, such as, ultrasonic assisted turning, welding, milling, drilling, grinding. Ultrasonic assisted machining technology has been studied by many cited references. All of these studies analyze in different ways, concept, design and dynamics of set-up, characteristics and finite element modeling and comparison of cutting forces during machining processes. In this present review only one dimensional ultrasonic assisted turning has been discussed and some ultrasonic assisted machining related to ultrasonic assisted turning is discussed.

2.4 Some Other Vibration Assisted Cutting

Liu et al. [14] have performed experimental study on distinctiveness of ultrasonic vibration-assisted cutting of tungsten carbide material using a CNC lathe with CBN tool inserts.. The SEM observations on the machined work-piece surfaces and chip formation indicated that the critical condition for ductile mode cutting of tungsten carbide was mainly the maximum undeformed chip thickness when the tool cutting edge radius was fixed, that is, the ductile mode cutting can be achieved when the maximum undeformed chip thickness was smaller than a critical value. Corresponding to the chip formation mode (ductile or brittle), three types of the machined work-piece surfaces were obtained: fracture free surface, semi-fractured surface and fractured surface. It was also found that the cutting speed has no significant effect on the ductile chip formation mode.

Chen et al. [15] performed experimental study on turning W-Fe-Ni alloy by conventional turning and ultrasonically assisted turning. They found that in ultrasonic assisted turning, feed rate still has significant influence on surface roughness, next to important factors are vibration parameters, while the influence of depth of cut and cutting speed on surface roughness become less profound than others parameters. Comparing with CT, the surface roughness machined by UAT reduced by the range of 7.05%-30.06%. They observed that UAT can give smoother surface, but the residual stress is larger than that in CT. It confirms that the rake surface of the vibration cutter has an intense ironing effect on the work piece surface.

Hsu et al. [16] study on the machining characteristics of Inconel 718 by combining ultrasonic vibration with high-temperature-aided cutting. Experiment is done using Taguchi experimental design to clarify the influence of various machining parameters on the machining characteristics. They found that the percentage contributions of the cutting tool, feed rate, working temperature and depth of cut for surface roughness are 33.16, 25.00, 13.36 and 9.17, respectively and the percentage contributions of the cutting speed, feed rate, cutting tool and depth of cut for cutting force are 22.27, 16.88, 13.80 and 13.37, respectively and also found that Ultrasonic-aided cutting improved the surface roughness by 9.10–51.61%, as well as decreasing cutting force by 32.34–24.47%. As a result, ultrasonic-aided cutting can enhance the cutting quality of Inconel 718.

2.5 Finite element study on ultrasonic assisted turning

S. Amini et al [17] studied machining of IN738 with a tool vibrating at ultrasonic frequency. The machining forces and stresses acting on the work-piece during the process, and the effect of process parameters such as cutting speed, tool geometry and vibration amplitude were investigated.

The results indicate that the forces and the stresses acting on the workpiece follow periodic changes during UAT and are augmented with an increase in the ultrasonic vibration amplitude or the cutting speed.

B.C.Behera and S.K.Sahoo [18] proposed that, the primary function of the horn is to amplify the vibration of the tool to the level required for effective machining, but it serves also as a means of transmitting the vibrational energy from the transducer to the work piece: It does so by being in resonance with the transducer. The design and manufacture of the horn require special attention because an incorrectly manufactured horn will damage machining performance and can lead to the destruction of the vibration system and cause significant damage to the generator. Horns are generally made of metals that have high fatigue strengths and low acoustic losses. The metals most often used to construct horns are titanium, carbon steel, stainless steel, heat treated steel and aluminum. Horns can be manufactured in various shapes and size. They are all of circular cross-section. An important aspect of horn design is the calculation of the correct resonant length, which length should usually be in multiples of half the wavelength of the system. The calculation of the resonant length is relatively simple for the exponential design. This design also gives good matching in terms of amplification. However, it is difficult to manufacture and is seldom used, unless necessary. It is also easy to calculate the resonant length for the stepped shape. This design gives high amplification but tends to have stress concentrations at the junction where the cross-section changes. Stress concentrations can lead to overheat and the formation of cracks and the alternating stresses developed are also greater. Thus stepped horns are used only when the end-face amplitude is small. The sharp corners are usually rounded to reduce stress concentrations, with little effect on the machining rate. The conical design is the most difficult in terms of calculating the resonant length, but it can be manufactured easily. It has as good amplitude matching as the exponential type and is thus used commonly.

2.6 Summary

This chapter has presented a literature survey with a critical review on one dimensional ultrasonic assisted turning. Different ultrasonic assisted turning set up, previous experimental and finite element study on ultrasonic assisted turning has been discussed. The mechanism of one dimensional ultrasonic assisted turning is also discussed.

The previous works presented are adapted and improved to produce a novel idea in ultrasonic assisted turning system development and its applications by using piezo-actuator as a vibration generator. Experiments have been conducted and obtained data are analyzed statistically.

Chapter 3

3. DESIGN AND FINITE ELEMENT MODELING OF UVT

3.1 Introduction

Ultrasonic vibratory tool (UVT) is an element operating in a longitudinal mode used for efficient transfer of ultrasonic energy from a source element (transducer) to a second horn, coupler, tool, or load. Equivalently, it is a transmission line, generally (but not always) providing a change of amplitude of vibration between the input and the output ends of the horn. The main purpose of the horn is to provide amplitude of vibration at its output end that is greater than that at the input end.

3.2 Horn length calculation

3.2.1 Exponential shape

The resonant length of a horn with the exponential shape is given by

$$L = \frac{C}{F}\sqrt{\left[1 + \left(1n\ \frac{N}{2\,\pi}\right)^2\right]} \tag{3}$$

Where C is the wave speed, f is the natural frequency of the machine and N is the diameter ratio D_1/D_2, which is also equal to the amplitude ratio. D_1 and D_2 are the diameters of the input and output ends of the horn, respectively. The wave speed C can be calculated using

$$C = \sqrt{\frac{E}{\rho}} \tag{3.1}$$

3.2.2 Stepped shape

The resonant length of the horn of stepped shape is given by

$$L = K_1 \frac{C}{4f} + K_2 \frac{C}{4f} \tag{3.2}$$

To simplify the calculation, it is usual to assume the correction factors k1 and k_2 be unity.

Hence,

$$L = \frac{c}{2f} \tag{3.3}$$

3.3 Vibratory Tool Equation and its Specific Solution

3.3.1 Plane wave equation

Let us consider the motion of plane wave in a velocity of sound, C, and attenuation of the waves is assumed to be zero. The waves are free to move in both the positive and negative directions of X-axis as described by Equation (3.4).

$$\xi = f_1(x - ct) + f_2(x + ct) \tag{3.4}$$

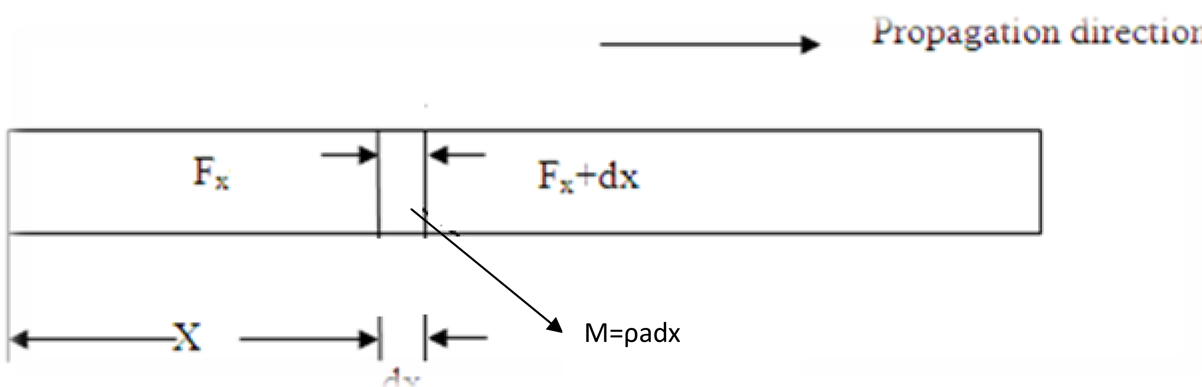

Figure 3.1 Forces on an increment normal to the direction of propagation of a longitudinal plane Wave in a uniform slender bar

Where, $f_1(x\text{-}ct)$ refers to waves moving in the positive direction of X-axis and $f_2(x+ct)$ to waves moving in the negative direction of X-axis. ξ is the displacement of dx . If *f(x-ct)* and *f(x+ct)* are continuous, Equation (3.5) may be differentiated twice with respect to x (keeping t constant), giving

$$\frac{\partial^2 \xi}{\partial x^2} = f_1^{''}(x - ct) + f_2(x + ct) \tag{3.5}$$

Similarly, differentiating Equation (3.5) with respect to t (keeping x constant)

$$\frac{1}{C^2}\frac{\partial^2\xi}{\partial^2 t} = f_1(\text{x-ct})+\text{f}_2(x+ct) \quad (3.6)$$

By comparing equations (3.5) and (3.6),

$$\frac{\partial^2\xi}{\partial^2 t} = C^2\frac{\partial^2\xi}{\partial^2 X} \quad (3.7)$$

The Equation (3.4) is the general solution of plane wave equation (3.7). The characteristics of a true plane wave are that pressure and motions at every position in a plane normal to the direction of propagation are equal in amplitude and phase. The kind of wave is not defined by the velocity 'C' in Equation (3.7). The bar is assumed to be so slender (D≫ λ) that the effects of poison' s ratio can be neglected is a specific example of Equation (3.7). Where λ the wavelength and D is the diameter of the bar.

Let us consider a uniform, narrow, homogeneous, elastic bar as being composed of series of incremental elements of density ρ, longitudinal thickness dx, and cross section area A (Figure 3.1). Losses are assumed to be negligible. Balancing the forces of momentum of an element

$$F_m = Ma_c = \rho A\frac{\partial^2\xi}{\partial x^2}dx \quad (3.8)$$

Where, *M=ρAdx*, ξ is displacement of the element dx, $a_c = \frac{\partial^2\xi}{\partial x^2}$ and t is the time against the elastic reaction of a neighboring element situated between x and (x+dx), in the same way using deriving spring equation,

$$F_{spring} = EA\frac{\partial^2\xi}{\partial x^2}dx \quad (3.9)$$

$$F_x = -EA\frac{\partial\xi}{\partial x} \qquad F_{x+dx} = dF_x\frac{dF_x}{dx}dx$$

From Figure 3.1 F_m=F_{spring}

So $$A\frac{\partial^2\xi}{\partial x^2}dx = EA\frac{\partial^2\xi}{\partial x^2}dx \quad (3.10)$$

Or $$\frac{\partial^2\xi}{\partial t^2} = \frac{E}{\rho}\frac{\partial^2\xi}{\partial x^2} = C^2\frac{\partial^2\xi}{\partial x^2} \quad (3.11)$$

Where $$C = \sqrt{\frac{E}{\rho}} \quad (3.12)$$

C is the velocity of sound and E is young's modulus of elasticity in the medium of the bar.

3.3.2 Plane wave equation of tapered horn

Similarly, the wave equation of tapered horn (Figure 3.2) in terms of particle displacement, ξ is,

$$\frac{1}{C^2}\frac{\partial^2\xi}{t^2} - \frac{1}{A}\frac{\partial A}{\partial x}\frac{\partial\xi}{\partial x} - \frac{\partial^2}{\partial x^2} = 0 \quad (3.13)$$

And in terms of particle velocity, v, and implying harmonic motion,

$$\frac{\partial^2 v}{\partial x^2} - \frac{1}{A}\frac{\partial A}{\partial x}\frac{\partial v}{\partial x} - \frac{\omega^2}{C^2} = 0 \quad (3.14)$$

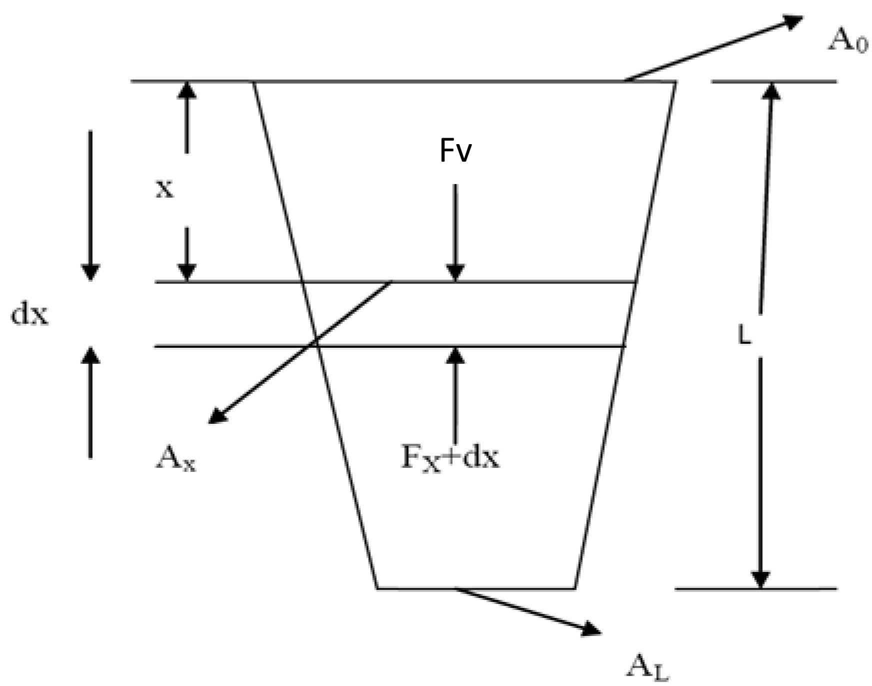

Figure 3.2 Propagation of longitudinal wave in a tapered horn [18]

3.3.3 Plane wave equation of stepped cylindrical horn or vibratory tool

For uniform cross section bar $\frac{\partial A}{\partial x} = 0,$

The equation of tapered bar (Equations 3.13 & 3.14) reduces to the plane wave equation for which the general solution, in terms of the displacement, ξ, will be

$$\xi = \left[A\cos\frac{\omega x}{c} + B\sin\frac{\omega x}{c}\right]\cos(\omega t) \tag{3.15}$$

or in terms of particle velocity

$$v = -\omega\left[A\cos\frac{\omega x}{c} + B\sin\frac{\omega x}{c}\right]\sin(\omega t) \tag{3.16}$$

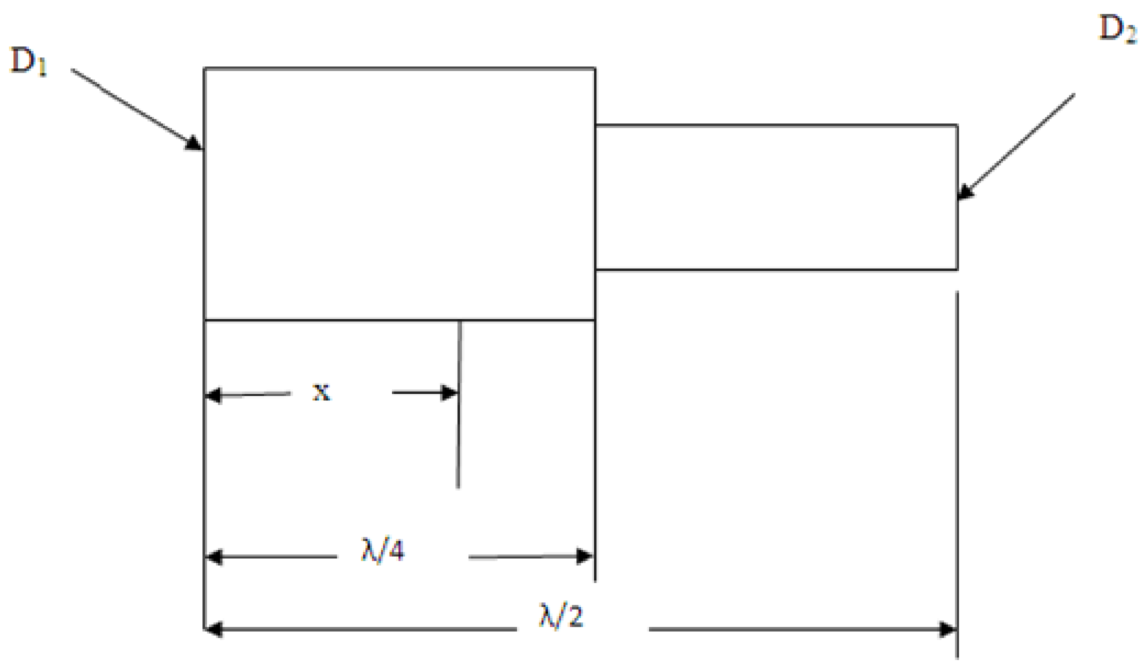

Figure 3.3 Stepped cylindrical half wave vibratory tool

For longitudinal half wave uniform bar (Figure 3.3)

$$\xi = \xi_M\cos\left(\frac{\omega x}{c}\right)\cos\omega t \tag{3.17}$$

$$v = -\omega\xi_M\cos\left(\frac{\omega x}{c}\right)\sin\omega t \tag{3.18}$$

Where ξ_M is a maximum displacement and is located at x=0. The acceleration at any point, x, along the tool is

$$a = -\omega^2 \xi_M \cos\left(\frac{\omega t}{c}\right) \cos\omega t = -\omega^2 \xi \tag{3.19}$$

Where λ is the wave length, ω is the angular velocity. Stress, s, at x in a half wave resonant bar is

$$s = \frac{iE}{\omega}\frac{dv}{dx} \tag{3.20}$$

Where $\omega\xi_m$ is the maximum velocity and occurs X=0, E is young' s modulus of elasticity, and $i = \sqrt{-1}$.

For the vibratory tool (Figure 3.3), with the step occurring at the mid plain along the length, momentum of the elements on either side of step leads to the identity

$$\frac{\xi_1}{\xi_2} = \frac{v_1}{v_2} = \frac{A_2}{A_1} \tag{3.21}$$

Where ξ_1 & ξ_2 are particle displacements (amplitude) at X=0 and X=L, v_1&v_2 the particle velocity at X=0 and X=L, A1&A2 is the cross sectional area at x= 0 and X=L.

Or, $$\xi_1 = \frac{A_2}{A_1}\xi_2 \tag{3.22}$$

ξ_1 & ξ_2 are the amplitudes at driving and driven ends of the vibratory tool.

3.3.4 Stress concentration at a step in horn

When double cylinders are used as a half wave vibratory tool with step at the node (λ/4), the maximum stress occurs at the step is calculated approximately by using the stress occurs at the step. The maximum stress is calculated approximately by using the stress in the smaller diameter sector. The stress at node is

$$s_m = E\frac{\omega\xi_1}{X\xi_2} = E\frac{\omega}{C}\frac{A_2}{A_1}\xi_1 \qquad (3.23)$$

A horn designed according to Figure 3.3 will fail in fatigue at the junction between the two elements. This junction is a position of maximum stress, and abrupt change in diameter increases the stress near the surface of the smaller diameter segment and the nodal face of the larger diameter. In practice, these horns are designed with a highly polished fillet located between the larger diameter and the smaller diameter segments to reduce the stress concentration at the junction. The concentration value, K, (Table 3.1) for various fillet radii can be determined by using the relationship [19] (Figure 3.4).

$$K = K_1 + K_2\left(\frac{2h}{D}\right) + K_3\left(\frac{2h}{D}\right)^2 + K_4\left(\frac{2h}{D}\right)^3 \qquad (3.24)$$

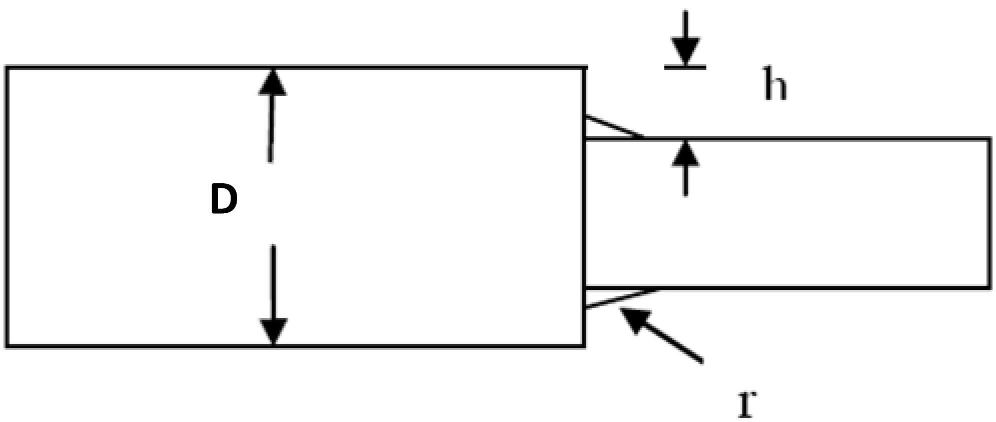

Figure 3.4 Double cylinders with square shoulder and fillet

Table 3.1 Concentration value (K) for various fillet radii [18]

	For 0.25 h/r 2.0	For 0.20 h/r 2.0
K_1	$0.927+1.149(h/r)^{0.5}-0.086h/r$	$1.225+0.831(h/r)^{0.5}-0.010h/r$
K_2	$0.011-3.029(h/r)^{0.5}+0.984h/r$	$-1.831-0.318(h/r)^{0.5}-0.049h/r$
K_3	$0.304+3.979(h/r)^{0.5}-1.737h/r$	$2.236-0.522(h/r)^{0.5}+0.176h/r$
K_4	$0.366-2.098(h/r)^{0.5}+0.875h/r$	-0.630+0.009(h/r)0.5-0.117h/r

The concentration stress, S_c, is

$$S_c = KS_m \tag{3.25}$$

Where S_m is the values of stress calculated using Equation 3.22.

3.3.5 Calculation of nodal plane in stepped cylindrical vibratory tool.

Locations of nodal planes are necessary to clamping the ultrasonic system. The plane where particle displacement of vibratory tool is zero is called nodal plane. For rigidity of the ultrasonic system it is better to clamp at nodal plane. Clamping the ultrasonic system other than nodal plane fluctuate the amplitude and frequency of the ultrasonic vibratory tool which affect the ultrasonic assisted tuning (UAT).

Referring Equation 3.17

$$\xi = \xi_M \cos\left(\frac{\omega x}{c}\right) \cos \omega t = 0 \tag{3.26}$$

(At nodal plane ξ=0)

$$\cos\left(\frac{\omega x}{C}\right) = 0 \tag{3.27}$$

$$x_n = \frac{nC}{4f} (\text{n} = \text{odd number}) \tag{3.28}$$

Where x is nodal plane position, f is frequency and C is velocity of sound.

3.3.6 Calculation of Tool Tip Amplitude

As shown in Figure (4.1), the cutting tool treated as a cantilever beam in this experiment. The vibratory tool is placed 35mm from the fixed end and cutting tip is 70mm from the fixed end. The output amplitude of vibration of UVT is 8µm.

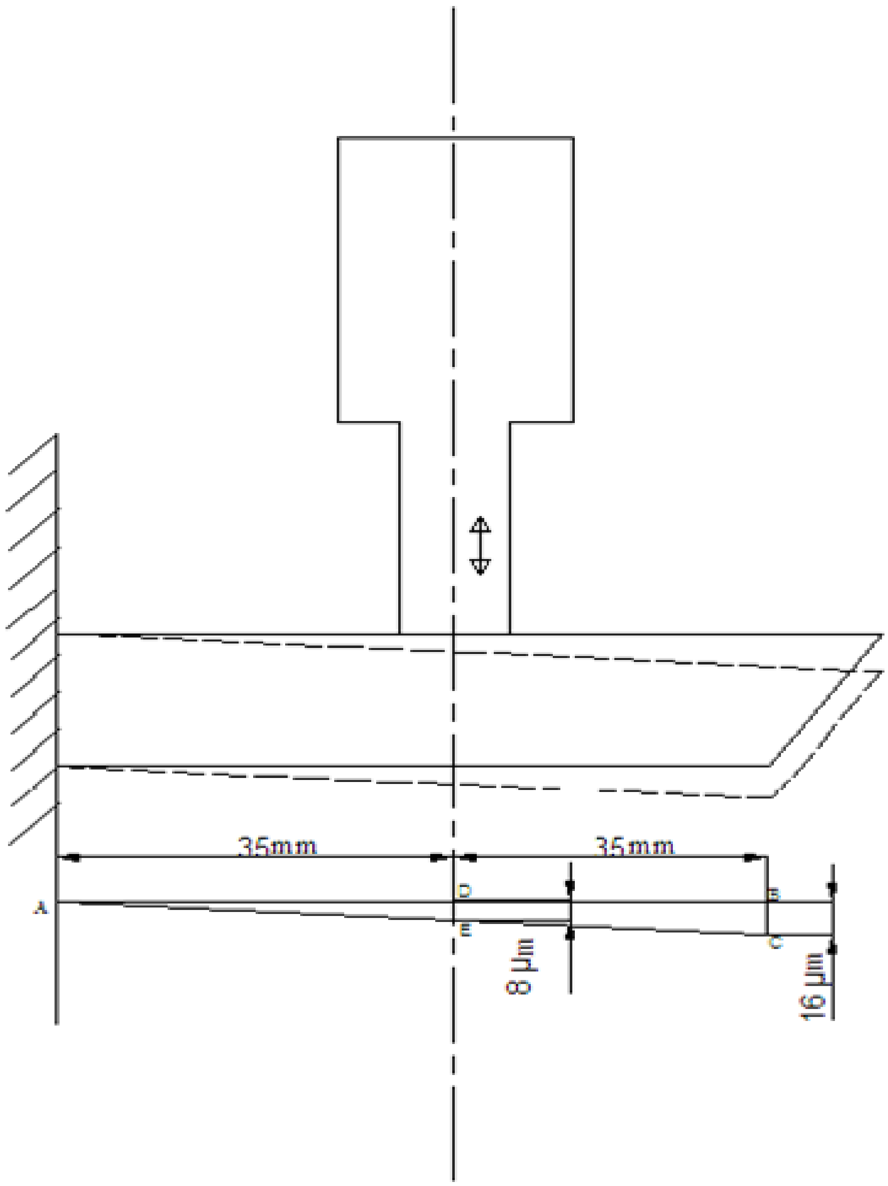

Figure 3.5 Cutting tool during ultrasonic vibration (treated as a cantilever beam) [20].

From Figure 4.1 (using triangular rule)

$$\Delta DAE \cong \Delta ABC$$

$$\text{Or} \quad \frac{BC}{DE} = \frac{AB}{AD}$$

$$\text{Or} \qquad BC = \frac{AB}{AD} DE$$

$$BC = 16\mu\text{m}$$

BC is the amplitude of vibration of cutting tip.

3.4 Finite Element Modeling of Ultrasonic Vibratory Tool

3.4.1 What is Finite Element Analysis?

FEA consists of a computer model of a material or design that is stressed and analyzed for specific results. It is used in new product design, and existing product refinement. A company is able to verify a proposed design will be able to perform to the client's specifications prior to manufacturing or construction. Modifying an existing product or structure is utilized to qualify the product or structure for a new service condition. In case of structural failure, FEA may be used to help determine the design modifications to meet the new condition.

3.4.2 A Brief History of Finite Element Analysis

Finite Element Analysis (FEA) was first developed in 1943 by R. Courant, who utilized the Ritz method of numerical analysis and minimization of variation calculus to obtain approximate solutions to vibration systems. Shortly thereafter, a paper published in 1956 by M.J. Turner, R.W. Clough, H.C. Martin, and L.J. Topp established a broader definition of numerical analysis. The paper centered on the "stiffness and deflection of complex structures".

By the early 70's, FEA was limited to expensive mainframe computers generally owned by the aeronautics, automotive, defense, and nuclear industries. Since the rapid decline in the cost of computers and the phenomenal increase in computing power, FEA has been developed to an incredible precision. Present day supercomputers are now able to produce accurate results for all kinds of parameters.

3.4.3 Modeling pre-processor

Finite element analysis is performed by using the commercial package ANSYS which is one of the most powerful and flexible tools for available for dynamic analysis of structures. As far as we know, the finite element method is very useful in finding the resonance frequency and analyzing the vibration displacement distribution of acoustic horn with any dimension. In this finite element analysis, the major factors used for modeling a general structural pressure simulation included element type, real constant, material properties, geometry, meshing, boundary conditions, etc. After these factors have been set, the analysis may begin. The factors for analysis of an ultrasonic horn are modal and harmonic analysis.

3.4.4 Geometry generation

The geometry (Figure 3.6) is generated in preprocessor modeling. The length of the horn is the resonance length (120mm).The input and output diameter is 40 and 20mm, tool length 20mm and width 5mm and fillet dimension (h/r) is taken 2 (Table 3.1).

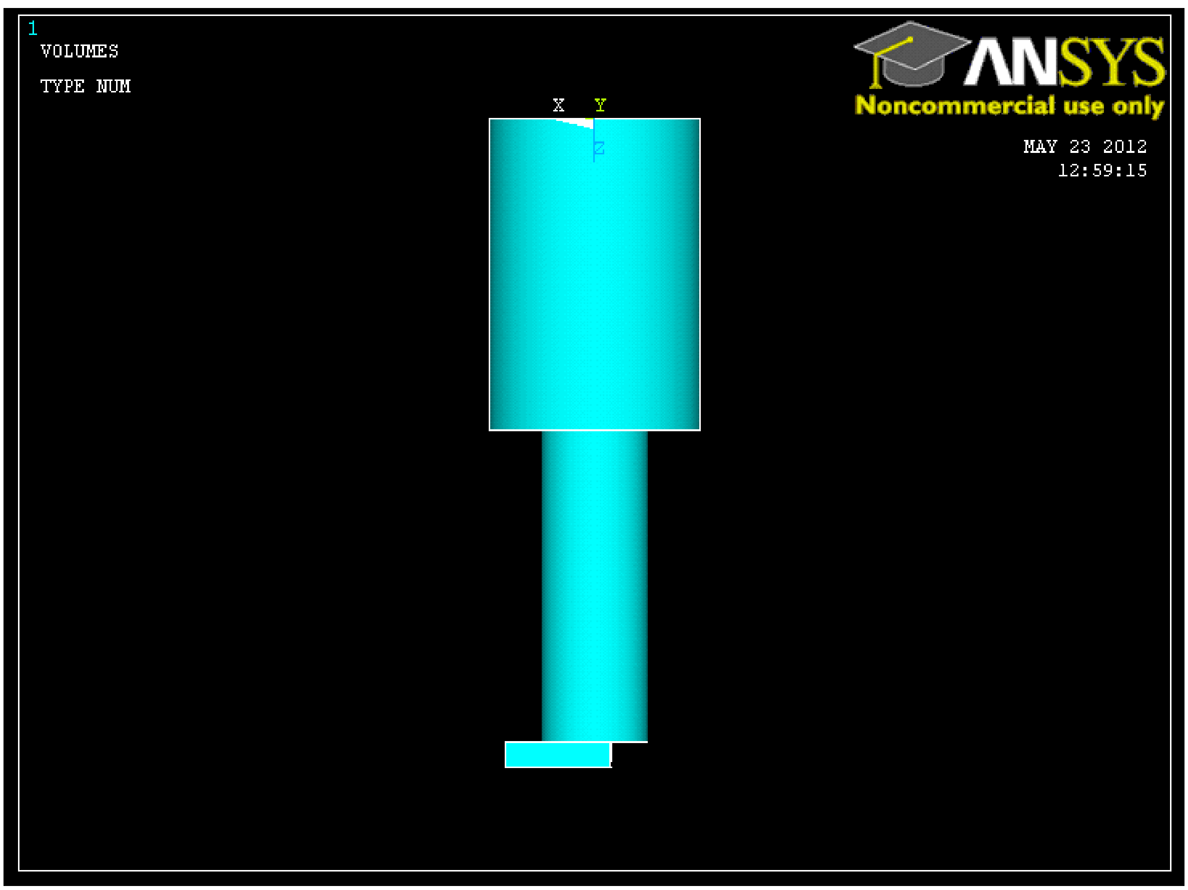

Figure3.6 Horn preprocessor model

3.4.5 Material properties

The titanium is used as the horn material for the analysis with properties, elastic modulus E= 110 GPa, Poisson's ratio, γ=0.33, mass density ρ= 4700 Kg/m^3. Tool steel is used as the single point cutting tool for the analysis with properties, elastic modulus E=210 GPa, Poisson's ratio γ=0.30, mass density ρ=8150kg/m^3.

3.4.6 Element type selection

Selection of suitable element types according to material and design of the UVT are made to ensure the analytical correctness. The UVT is predominantly divided into metallic materials. Element selection varies due to differing features. Considering the special curved surface structure of the vibrating system, solid 92, a tetrahedron with 10 nodes Figure (3.6) is selected as the element. As the tetrahedron element allows the finite element analysis software to grid a complex geometric model easily, it is considered to be suitable for the shape requirement of the vibrating tool.

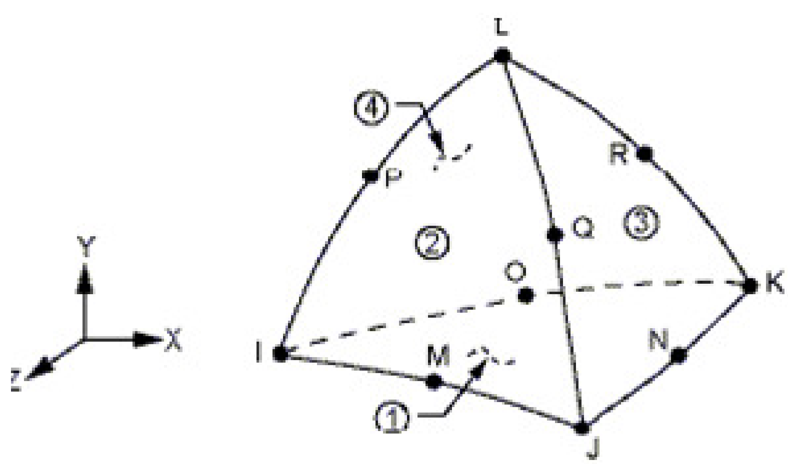

Figure 3.7 Solid 92 elements [reproduced from ANSYS 12.0 user guides [19]]

3.4.7 Mesh generation

According to the basic principles of finite element analysis theory, the smaller the mesh element size is, the more accurate the results of an analysis will be. If the mesh element sizes infinitely small, the theoretical model will approach the optimal solution. However, this is only a presupposition. In the analysis process, when elements are too small, element meshing will generate too many elements, nodes and freedom for the model in general. This increases computational intensity, resulting in a model that is either too time-consuming to solve, or potential errors in values. Thus, reasonable mesh element size (number of elements) is a factor that should be considered in a finite element analysis. In the present analysis 14491 numbers of elements with 21517 nodes are used for the model. Figure (3.8) shows the mesh generation modal.

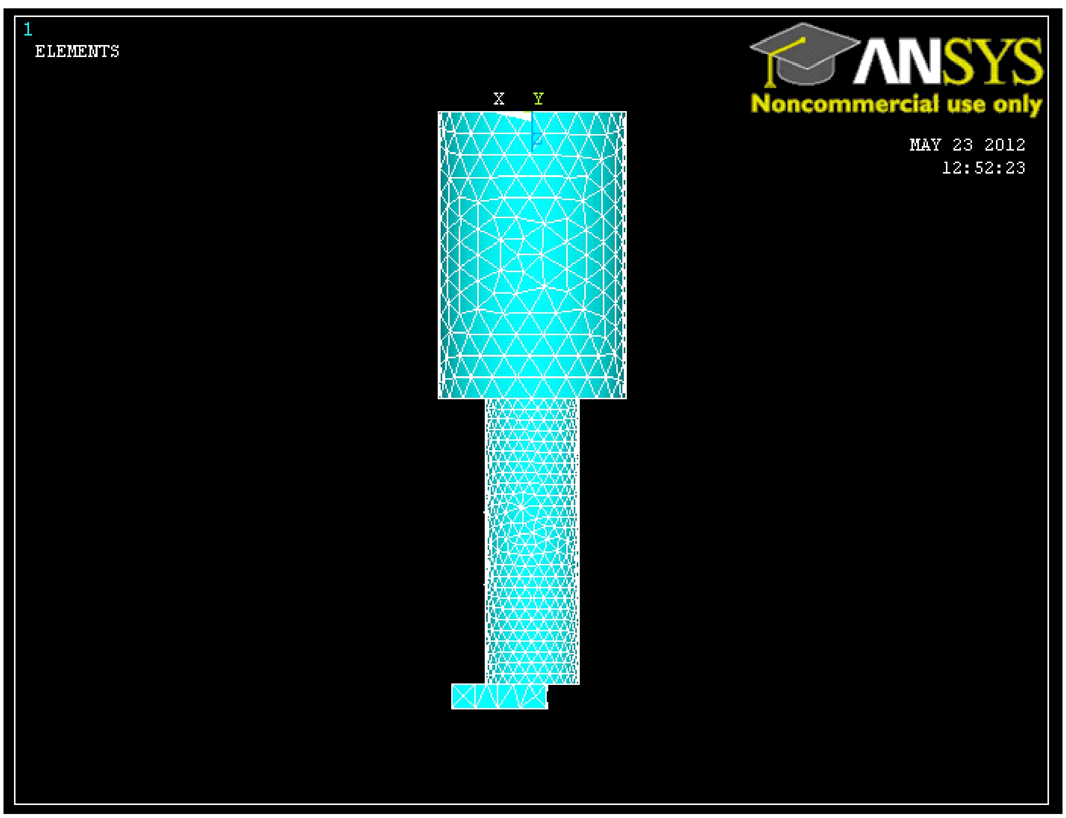

Figure3.8 Mesh generation of horn

3.4.8 Boundary condition

After finalizing settings for the ANSYS® pre-processor, boundary conditions are provided to the solution-finding processor. The output of piezoelectric transducer is applied as input of tool. 0.01mm displacement uniformly distributed loads is applied at the big end of the ultrasonic vibrating tool as shown in Fig 3.8.

3.5 Results and Analysis

3.5.1 Modal analyses

Modal analysis allows the design to avoid resonant vibrations or to vibrate at a specified frequency. It helps in calculating solution controls for other dynamic analyses, because a structure's vibration characteristics determine how it responds to any type of dynamic load; always perform a modal analysis first before trying any other dynamic analysis. Modal analysis is a linear analysis, any nonlinearities such as plasticity and contact elements, are ignored, even if they are defined. Several mode extraction available in the modal analysis but in present case BLOCK LANCZOS extraction method is selected shown in Fig 3.9.

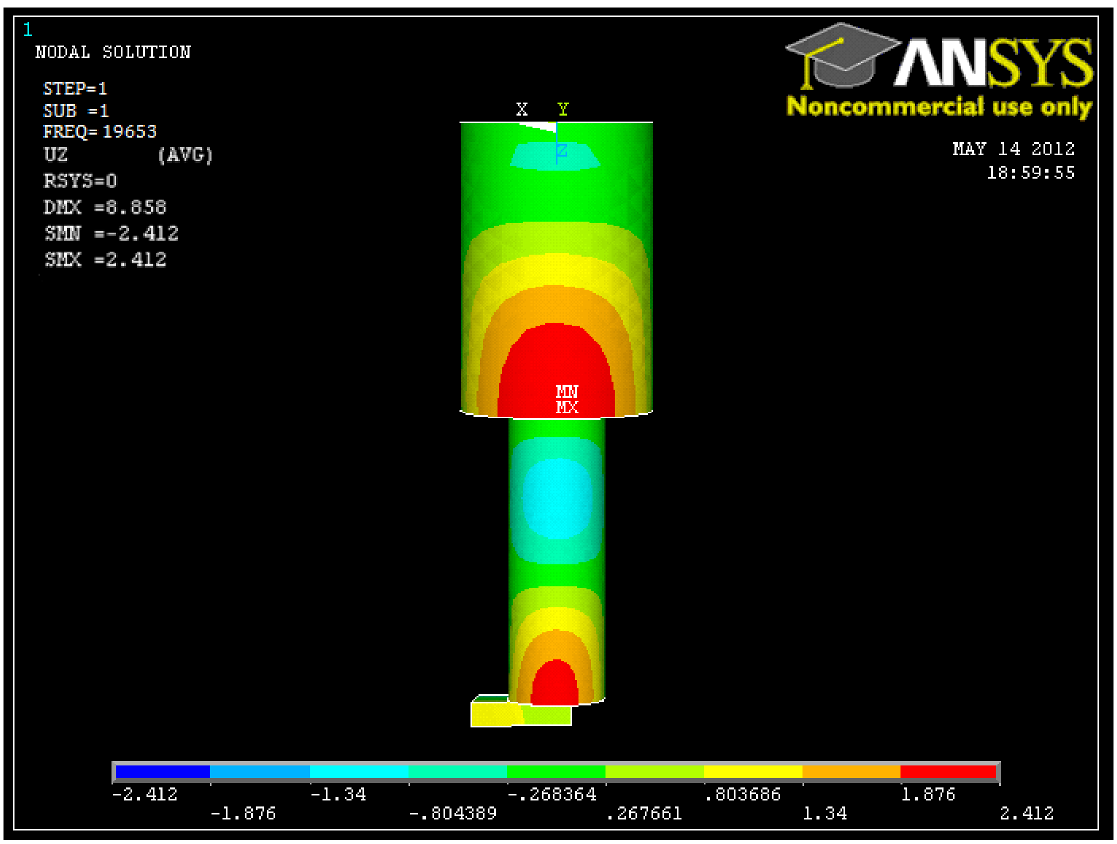

Figure3.9 Modal analyses of UVT

The results of modal analysis show that used horn configuration gives definite and wide nodal band for clamping purpose. In modal analysis the frequency is generating 19653Hz and out-put amplitude is 4 times greater than input amplitude.

3.5.2 Harmonic analyses

The technique to determine the steady state response of a structure to sinusoidal (harmonic) loads of known frequency where the input harmonic loads are forces, pressures, imposed displacements, and imposed voltage of known frequency. The output parameter is harmonic displacement at each DOF, current flow for piezoelectric elements, stresses and strains.3. Methods of solving the harmonic equation of motion, but in present case Full method is selected, it is uses in full structure and unsymmetrical matrices (ultrasonic stepped horn) shown in Figure 3.10.

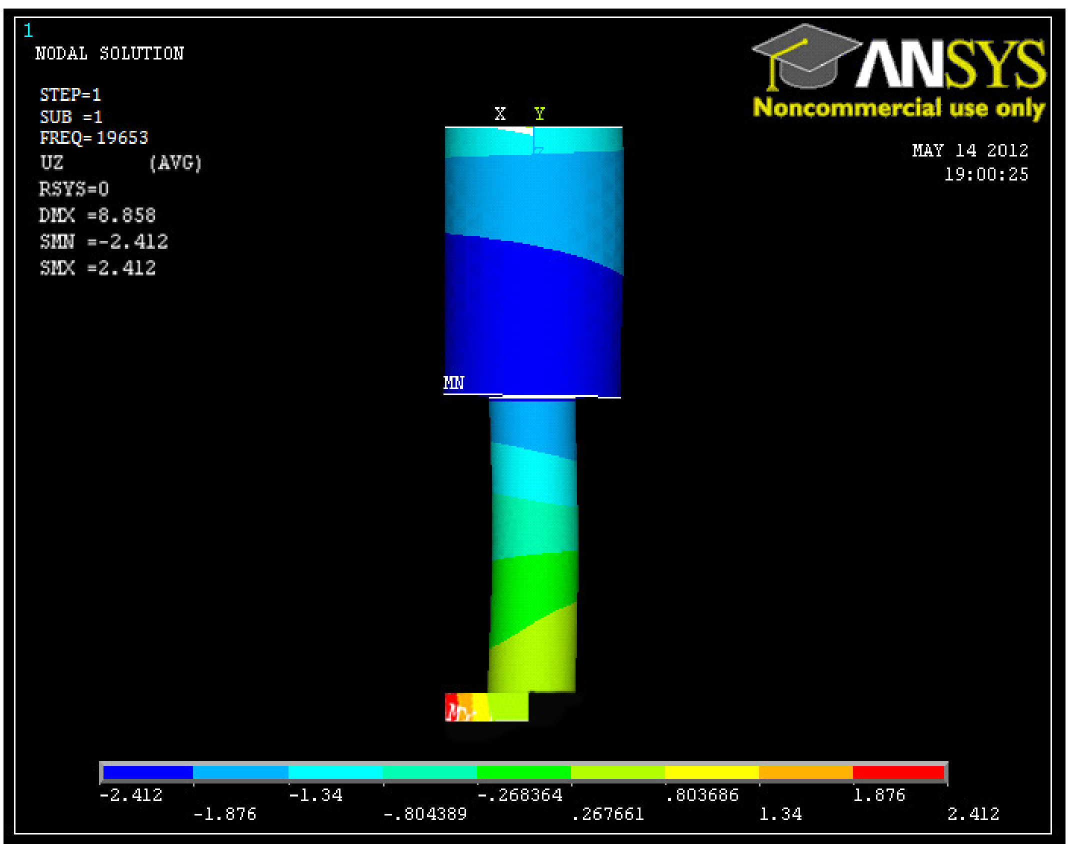

Figure3.10 Harmonic analysis of UVT

An additional point to be considered when designing UAT setup is that the horn should have at least one natural frequency within the allowable ultrasonic frequency, in this case 19653 Hz (19,500–20,500 Hz). It can be concluded that the geometrical dimension and material properties of UVT used in analysis of horn can deliver the required frequency. This frequency is match with other part of the ultrasonic system and the resonance frequency of the horn under the generator frequency and the UVT is amplified 4 times of source amplitude to working amplitude.

Table 3.2 Dynamic Analysis of UVT

Horn material			Titanium				
D1	D2	Fillet dimension (h/r)	Resonance length	Driving amplitud e	Nodal point x_n	Amplitude at working end (theoretical)	Amplitude at working end (ANSYS®)
40mm	20mm	2	120mm	0.01mm	60.275mm	0.04mm	0.02412mm

Analysis type	step	Sub step	Natural frequency	Figure no.
Modal analysis	1	1	19653	3.9
Harmonic analysis	1	1	19653	3.10

3.6 Summary

It is very important to know the amplitude at every point of the ultrasonic horn, because: it allows precise determination of the nodal plane position for locking in place of the ultrasonic system for desired processing. The results of modal analysis show that used horn configuration gives definite and wide nodal band for clamping purpose. An additional point to be considered when designing UAT setup is that the horn should have at least one natural frequency within the allowable ultrasonic frequency, in this case 19653 Hz (19,500–20,500 Hz).

Chapter 4

4. EXPERIMENTAL PROCEDURE

4.1 Experimental set-up and procedure

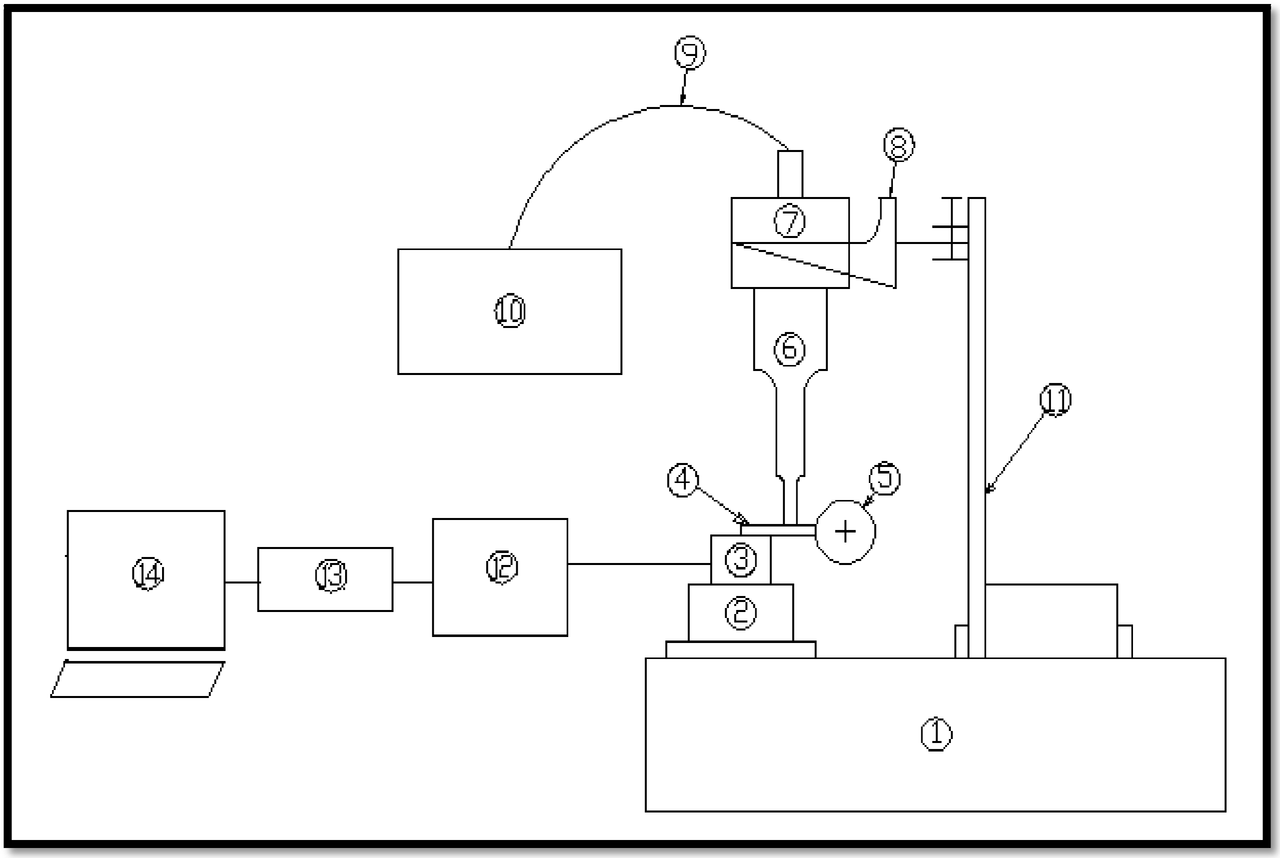

Figure 4.1 Schematic diagram of ultrasonic assisted turning

1. HMT Model NH 26 Lathe.
2. Compound plate
3. Dynamometer (Kistler model 9272)
4. Tool (treated as a cantilever)
5. Work-piece
6. Ultrasonic vibratory tool (UVT)
7. Booster/converter
8. Bracket

9 H.F.Cable with 4 pin coaxially (M) to (F) connector connects 20 kHz high voltage to converter.

10 Generators

11L-type holder

12 Charge amplifier model 5070A

13 DAQ

14 PC (CONTROL UNIT)

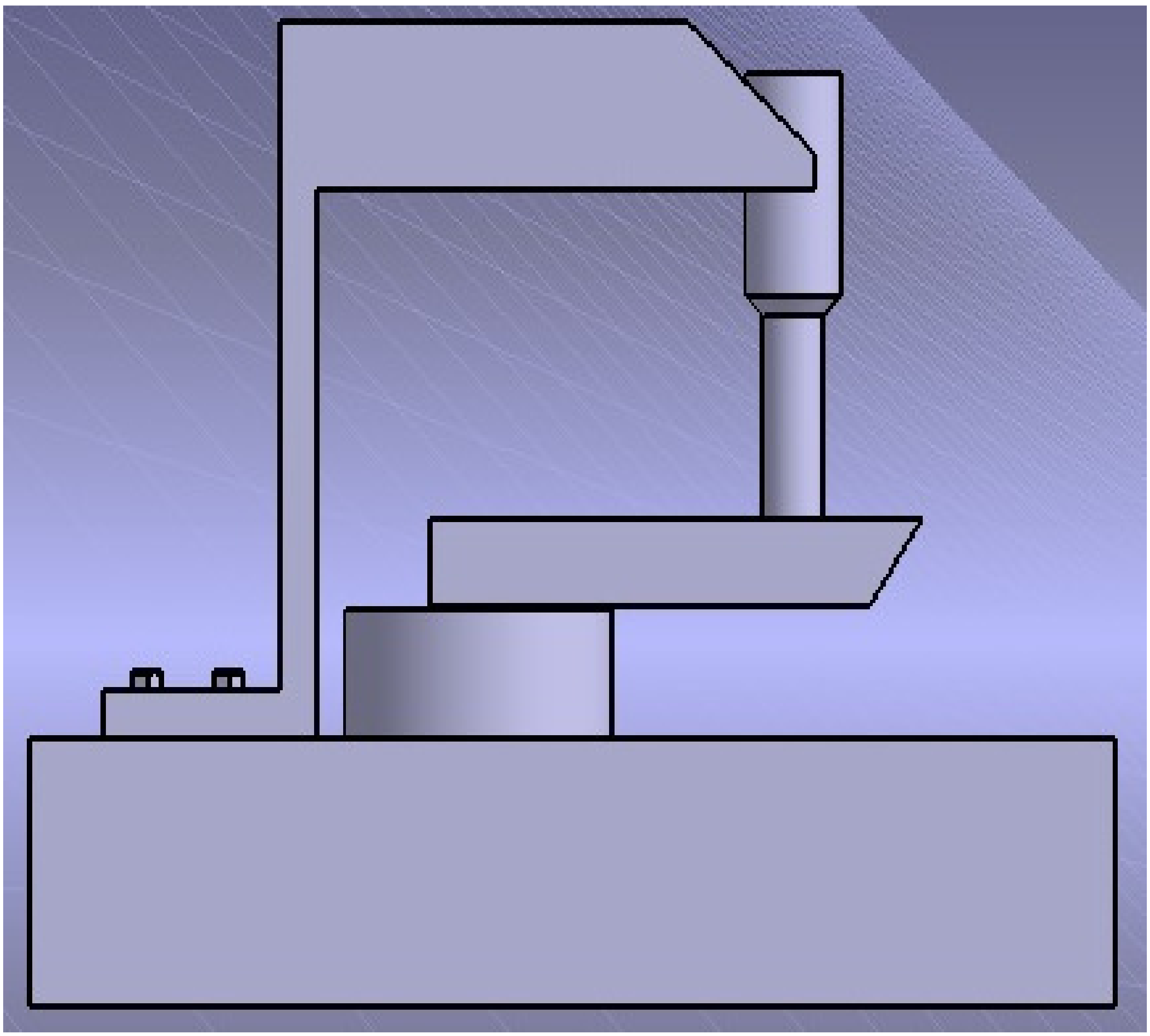

(a)

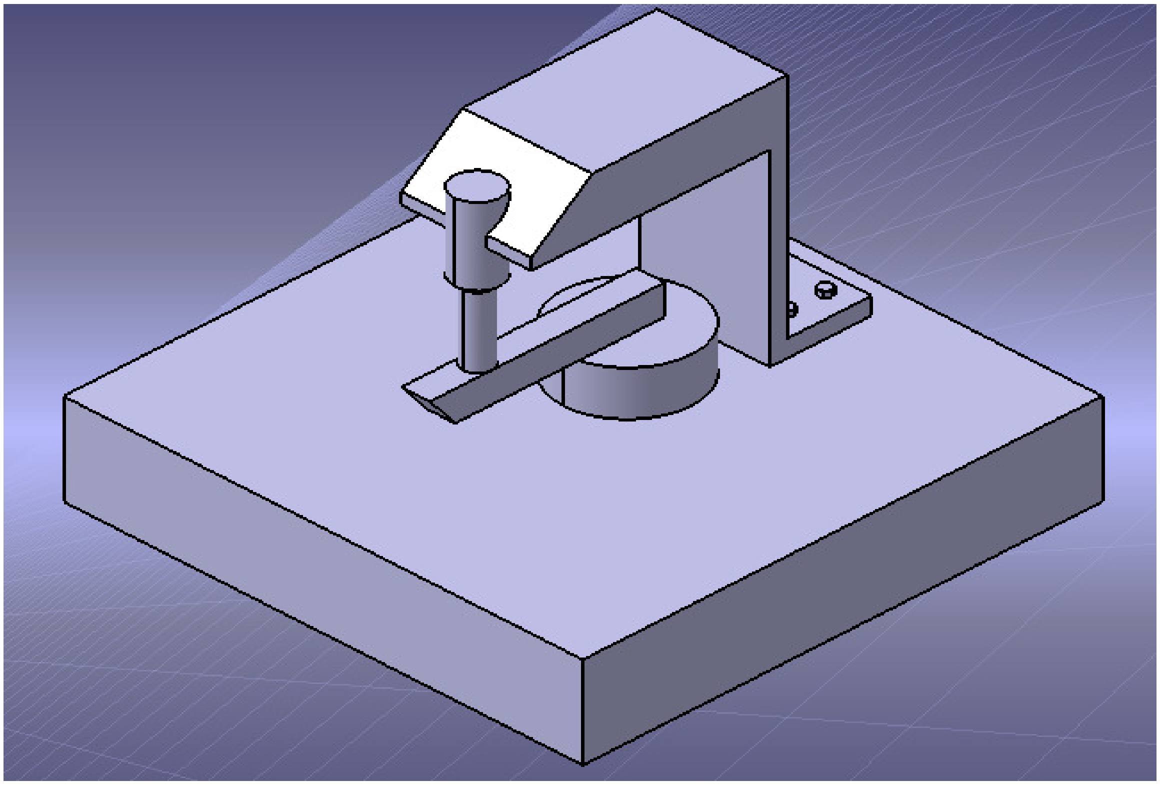

(b)

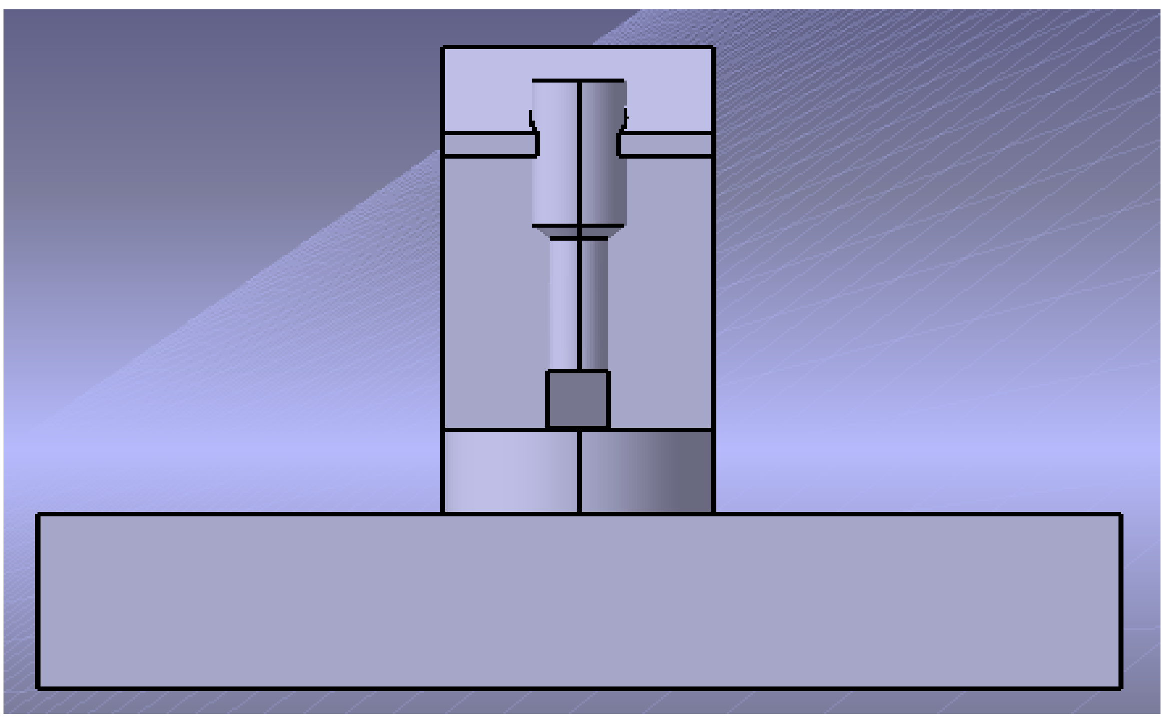

(c)

Figure 4.2 3D views of experimental set up (Cutting tool treated as cantilever beam). (a) Side view (b) Isometric view (c) Front view.

Figure 4.1 shows a schematic diagram of the ultrasonic vibration turning system used in the present experiments. This all experiments carried out HMT model NH 26" lathe. The commercial piezoelectric transducer (unloaded 20±0.5 kHz frequency) provides vibration to the ultrasonic vibratory tool (UVT). The tip of UVT is placed vertically on the cutting tool shown in Fig (4.1). The cutting tool is treated as a cantilever beam as shown in Figure 4.1, which is fixed on Kistler model 9272 dynamometer. Special designed L-shape holder maintained the height of the ultrasonic transducer shown in Fig (4.2), which is fixed on cross slide of the lathe. The UVT is connected to generator is generating high frequency around 20 ±0.5kHz.

The ultrasonic transducer is clamped at its nodal point by a light weight bracket and the bracket is fixed by sliding mechanism with special designed L-shape holder. This L-shaped holder maintained the height of the ultrasonic transducer, which is fixed on cross slide of the lathe. The UVT is connected to generator by H.F. Cable with 4 pin coaxially (M) to (F). The generator is generating high frequency around 20±0.5kHz with 2.0kW (max) power from the input mains voltage 230V AC, 50Hz frequency.

4.1.1 Cutting condition

Cutting condition used in machining work pieces is given in Table 4.1. The cutting is in dry state, the presented value was chosen to investigate the effect of superimposed ultrasonic vibration.

Table 4.1 cutting condition used in experiment

Work-piece material	S(m/min)	D(mm)	f(mm/rev)	d(mm)
Stainless steel(SS304)	57	45	0.04	0.1
	74	45	0.05	0.15
	96	45	0.06	0.2
	125	45	0.07	0.25

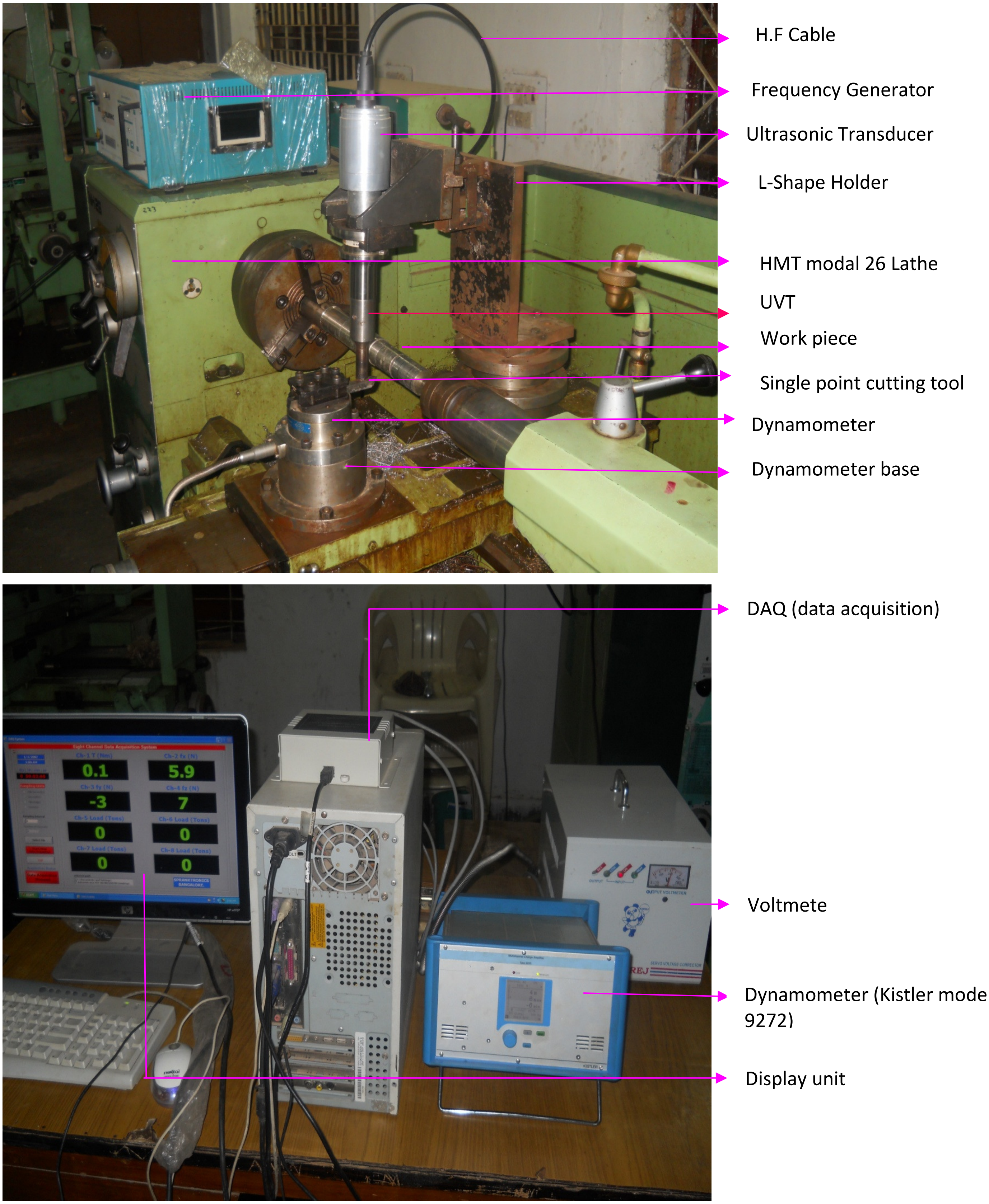

4.3 Experimental set-up of UAT

4.1.2 Specifications of total experimental set-up

Table4.2 Composition of work-piece (Stainless steel 304)

Composition of stainless steel 304	Fe	Cr	Ni	Mn	N	S	C	Si	P
percentage	64.99-74%	18%	8%	2%	0.10%	0.03%	0.08%	0.75%	0.045%

Table4.3 cutting tool geometry

material	Rake angle	Clearance angle	Cutting edge angle	Nose radius
Tool steel	0^0	24.932^0	43.631^0	0.2mm

Table4.4 Specifications Ultrasonic systems

Line voltage	220V/230V AC Single phase
Input frequency	50Hz
Current consumption	220V, 50Hz.-6A
Output frequency	20kHz
Amplitude	8µm
Output power	2kW
Output control	Auto tuning with load output power range 30 to 100% of nominal converter amplitude.
Operational mode	Continuous mode:-on/off & timer mode.
Tuning	Auto tuning operation in normal mode. Also manual tuning facility.
Converter weight with horn	Approx 1 Kg
Generator weight	Approx 3 Kg

Table4.5 Specification of UVT

Material	Titanium
Geometry (D_1-D_2-L)	40mm-20mm-120mm
Young's modulus (E)	110Gpa
poisson's ratio (γ)	0.33
Density (ρ)	4700
Natural frequency (f)	19700Hz

Table 4.6 Specifications of Kistler model 9272 dynamometer

Measuring range	
Force/moment	Range
F_X	-5-5kN
F_Y	-5-5kN
F_Z	-5-5kN
M_Z	-200-200N-m

Table 4.7 Specifications of control unit

Processor	Pentium 4
RAM	526 MB
Operating system	Windows XP
Screen resolutions	800 600 pixels

Table 4.8 Specifications of Data acquisitions (DAQ)

-National Instrument make USB based 14 bit 8 channels data card along with Lab view based data acquisition software to acquire the necessary parameters in the range of +/- 5V.

Table 4.9 Specification of single point cutting tool

Material	Tool steel
Geometry (D_1-W-L)	5mm-5mm-20mm
Young's modulus (E)	210GPa
Poisson's ratio (γ)	0.30
Density (ρ)	8150
Natural frequency (f)	19653

4.1.3 Work piece preparation and processing

Figure 4.4 Work piece after machining operation

The work-piece is cylindrical and faces are machined prior to the experiments. A finishing cut with a very small depth of cut is performed using the same cutting tool to be used in the experiments, in order to eliminate any leftover eccentricity. In the experimental run, first cut is made conventional and as soon as the tool travelled by 10mm the vibration is switched on thus allowing the second cut to proceed under same cutting conditions but with ultrasonic vibration. After finishing one experiment as shown in Figure 4.3, it is marked for identification. So, every experiment is divided two parts, first part is convention turning (CT) and second one is ultrasonic assisted turning (UAT). Each experiment was done at different cutting conditions and the same procedure is applied in different experiments.

4.2 Measurement of surface roughness

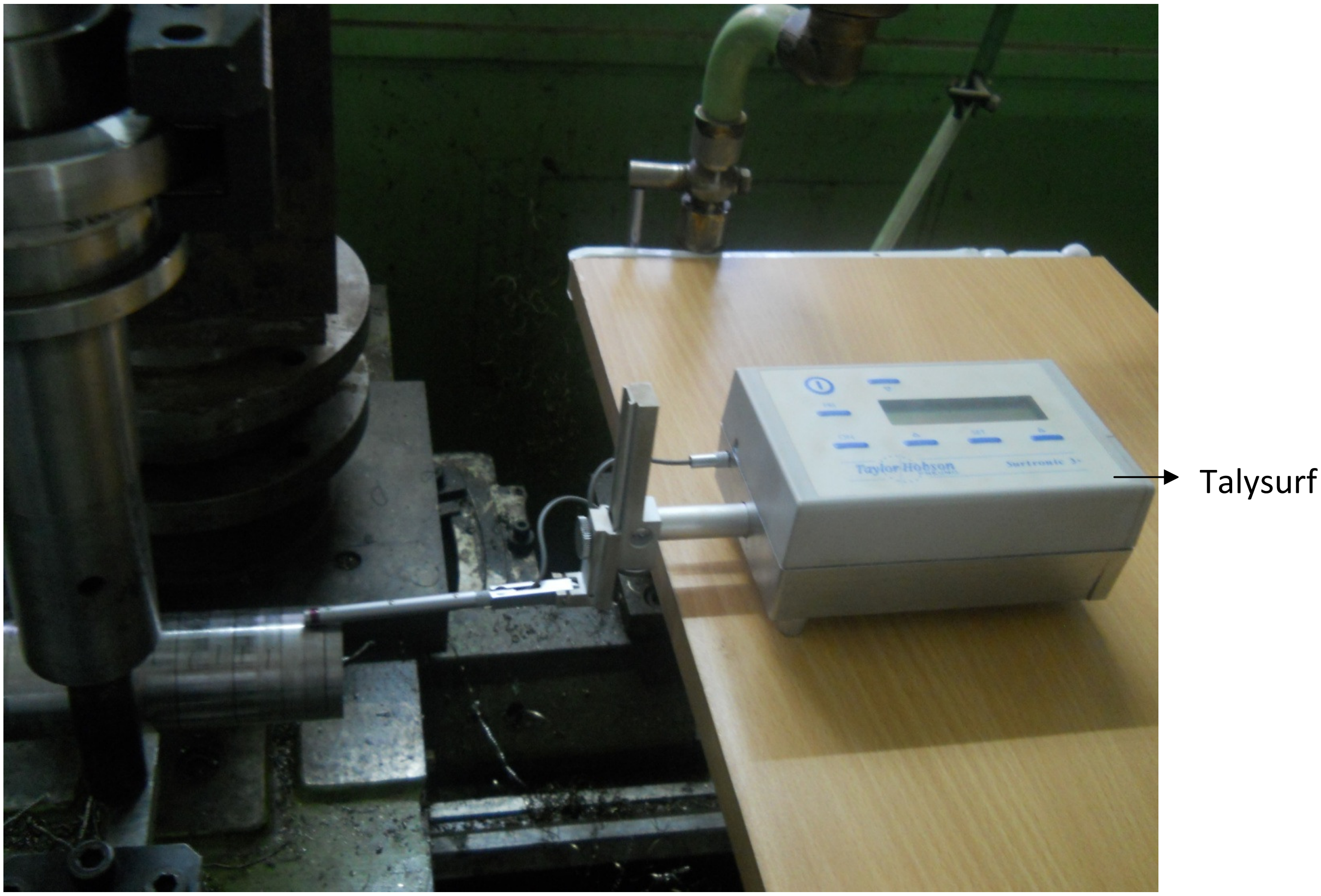

4.5 measuring surface roughness of the work-piece using Talysurf

Surface quality was assessed by measuring surface roughness along the axial direction of the work pieces. Both surfaces produced by application of ultrasonic vibration, and under conventional conditions, are evaluated using the “TALYSURF” surface measuring instrument. Centre line average (R_a) value is used to analyze the surface roughness of machined work-piece.

4.3 Measurement of cutting force

The Kistler model 9272 dynamometer (Table 4.6) is used to measure the cutting forces during experiments. The cutting tool is fixed on dynamometer and the dynamometer is fixed on the cross slide of the lathe. The dynamometer measures the active cutting force regardless of its application point. Both the average value of force and the dynamic force increase may be measured.

4.4 Result and Discussion

The bellow graphs can be drawn based on the experimental data shown in Table 4.10, on turning Stainless steel by conventional turning (CT) and ultrasonic assisted turning (UAT).

Table4.10 Design of experiment and out-put readings

Sl. No	Design of experiment (L_{16} orthogonal array)			Readings			
	d(mm)	f(mm/rev)	S(m/mm)	Ra©	Ra(u)	Fz©	Fz(u)
1	0.1	0.04	57	1.4	2	2902.72	4234.56
2	0.1	0.05	74	2.2	1	-78.59	-74.78
3	0.1	0.06	96	1.6	1.4	-43.99	-46.57
4	0.1	0.07	125	1.6	0.8	-8.12	-22.11
5	0.15	0.04	125	1.8	1.4	6311.06	6478.72
6	0.15	0.05	96	3.8	2	1303.9	6679.55
7	0.15	0.06	74	1.6	1.6	6168.31	6479.35
8	0.15	0.07	57	2.6	2.29	2634.37	8115.77
9	0.2	0.04	74	1.8	1.6	2784.72	4000.51
10	0.2	0.05	57	1.8	1.6	3766.42	1077.43
11	0.2	0.06	125	1.6	1	4561.55	5810.51
12	0.2	0.07	96	4.4	4.2	8817.31	1093.98
13	0.25	0.04	96	2.2	2	-2962.44	3431.54
14	0.25	0.05	125	1.2	0.8	3445.07	7024.54
15	0.25	0.06	57	2.2	2.2	1789.17	7181.99
16	0.25	0.07	74	2.6	1.8	2497.32	6822.81

4.4.1 Surface roughness in UAT and CT

Using TALISURF measuring the surface roughness in Ultrasonic assisted turning as well as conventional turning to the work-piece. UAT improved the surface roughness by 12.0–40.0% compare with conventional turning shown in Graph (4.1). It proves that UAT can obtain smoother surface.

Ra (c)-surface roughness in conventional turning

Ra (u)-surface roughness in ultrasonic assisted turning

4.4.2 Forces in UAT and CT

Using Kistler model 9272 dynamometer and control unit (Table 4.6&4.7) measuring the cutting forces on the work-piece both CT and UAT. The test results show that the cutting force for the UAT method decreases by 20.0–33.0 % in comparison with CT Graph (4.2). As a result, ultrasonic-aided cutting can enhance the cutting quality of Stainless steel.

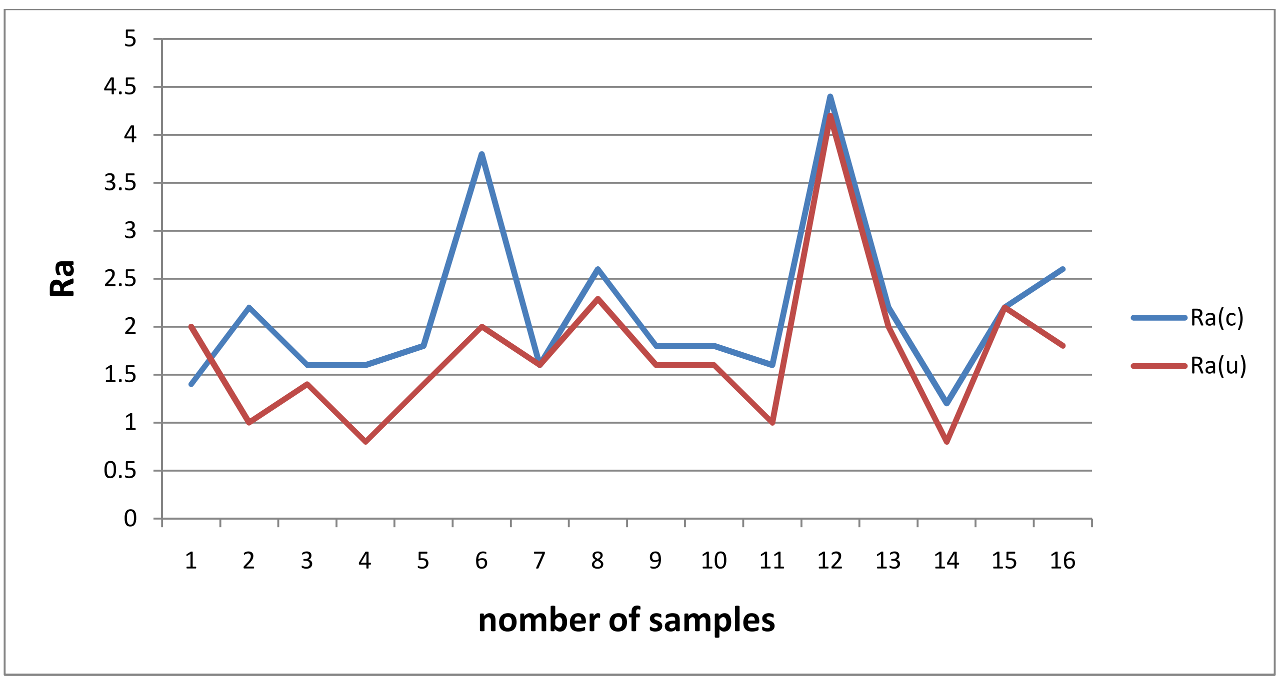

Graph4.1 Surface roughness in UAT and CT

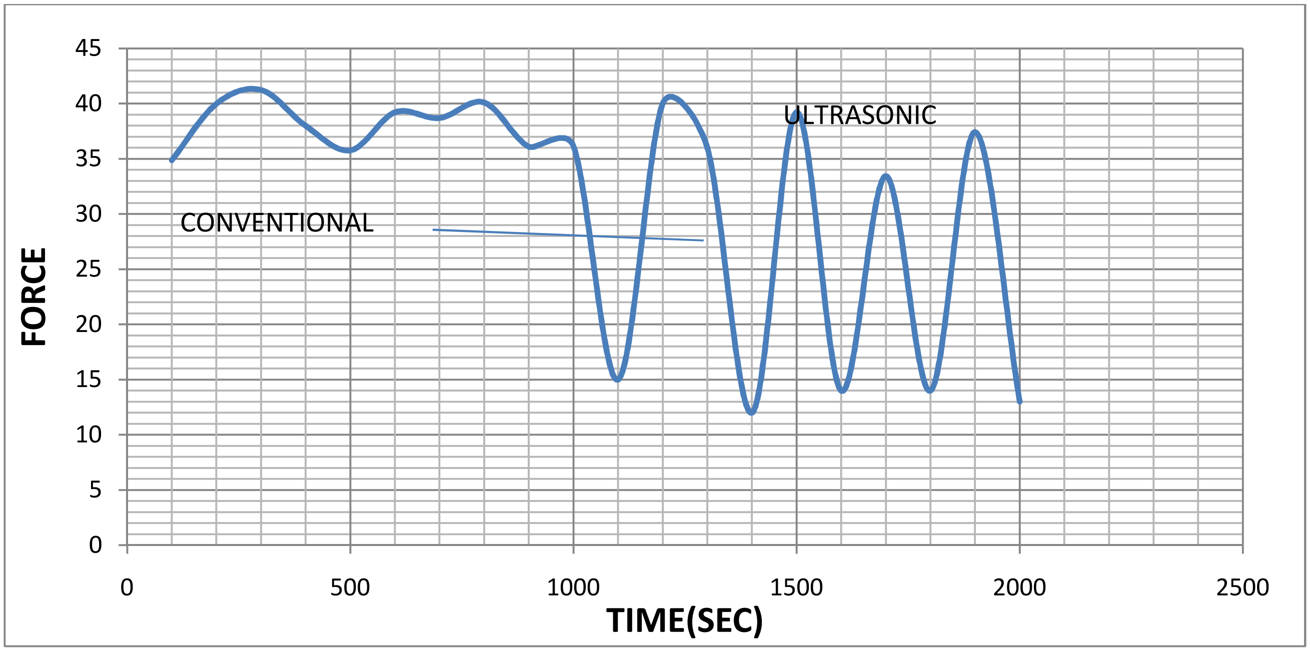

Graph 4.2 Forces in UAT and CT

4.5 Summary

The experimental study has carried out on turning Stainless steel by conventional turning (CT) and ultrasonic assisted turning (UAT). Because of the unstable turning process in CT, the surface can easily produce some defects such as burrs, tearing and so on, so the quality of surface becomes poor. While the UAT can reduce the influence of deformation and built-up-edge formation because of high frequency reciprocating movement between the contacting surfaces of the tool and the work piece, so as to make the turning process more stable. UAT improved the surface roughness by 12.0–40.0%. It proves that UAT can obtain smoother surface. The test results show that the cutting force for the UAT method decreases by 25.0–35.0 % in comparison with CT. As a result, ultrasonic-aided cutting can enhance the cutting quality of Stainless steel.

Chapter 5

5. OPTIMIZATION OF MACHINING PARAMETERS

5.1. Taguchi design

Dr. Genichi Taguchi is regarded as the foremost proponent of robust parameter design, which is an engineering method for product or process design that focuses on minimizing variation and/or sensitivity to noise. When used properly, Taguchi designs provide a powerful and efficient method for designing products that operate consistently and optimally over a variety of conditions. Taguchi proposed several approaches to experimental designs that are sometimes called "Taguchi Methods." These methods utilize two-, three-, four-, five-, and mixed-level fractional factorial designs. Taguchi refers to experimental design as "off-line quality control" because it is a method of ensuring good performance in the design stage of products or processes. In this process TOPSIS with TAGUCHI is used to optimize the out-put parameters [22].

5.1.1 Taguchi design experiments in MINITAB

MINITAB provides both static and dynamic response experiments in a static response experiment the quality characteristic of interest have a fixed level. The goal of robust experimentation is to find an optimal combination of control factor settings that achieve robustness against (insensitivity to) noise factors. MINITAB calculates response tables and generates main effects and interaction plots for,

- Signal-to-noise ratios (S/N ratios) vs. the control factors.
- Means (static design) vs. the control factors.

A Taguchi design or an orthogonal array the method is designing the experimental procedure using different types of design like, two, three, four, five, and mixed level. In the study, a three factor four level setup is chosen with a total of sixteen numbers of experiments to be conducted and hence the Orthogonal Array L_{16} was chosen. This design would enable the two factor interactions to be evaluated. As a few more factors are to be added for further study with the same type of material, it was decided to utilize the L_{16} setup, which in turn would reduce the number of experiments at the later stage. In addition, the comparison of the results would be simpler.

The levels of experiment parameters depth of cut (d), feed (f), and speed of the spindle (N) are design are shown in Table 5.1.

Table 5.1 Experimental Conditions and out-put responses

Factor	Code	Levels of factor			
		1	2	3	4
Depth of cut	d(mm)	0.1	0.15	0.2	0.25
Feed	f(mm/rev)	0.04	0.05	0.06	0.07
speed	S(m/min)	57	74	96	125

Sl.no	d(mm)	f(mm/rev)	S(m/min)	(Ra)u	fz(u)
1	0.1	0.04	57	2	4234.56
2	0.1	0.05	74	1	-74.78
3	0.1	0.06	96	1.4	-46.57
4	0.1	0.07	125	0.8	-22.11
5	0.15	0.04	125	1.4	6478.72
6	0.15	0.05	96	2	6679.55
7	0.15	0.06	74	1.6	6479.35
8	0.15	0.07	57	2.29	8115.77
9	0.2	0.04	74	1.6	4000.51

10	0.2	0.05	57	1.6	10774.46
11	0.2	0.06	125	1	5810.51
12	0.2	0.07	96	4.2	10937.98
13	0.25	0.04	96	2	3431.54
14	0.25	0.05	125	0.8	7024.25
15	0.25	0.06	57	2.2	7181.99
16	0.25	0.07	74	1.8	6822.81

5.2 TOPSIS

TOPSIS (technique for order preference by similarity to ideal solution) is a simple method which considered that the chosen alternative should have the shortest distance from the ideal solution and the longest distance from the negative ideal solution. Such an approach is both comprehensible and functional (Lee-ing Tong and Chao-Ton Su, [23]). According to Hwang and Yoon [24], the ideal solution is a hypothetical solution for which all attribute values correspond to maximum attribute values in the database comprising the satisfying solution; the negative ideal solution is a hypothetical solution for which all attribute values correspond to minimum attribute values in the database. TOPSIS thus gives a solution that is not only closest to hypothetically best, that is also the farthest from hypothetically worst (Lan, [25]).

For example, Let the Fuzzy **MADM** can be concisely expressed in matrix format as follows:

$$D = \begin{pmatrix} & X_1 & X_2 & X_3 & & X_n \\ A_1 & x_{11} & x_{12} & x_{13} & \dots & x_{1n} \\ A_2 & x_{21} & x_{22} & x_{23} & \dots & x_{2n} \\ \vdots & \vdots & \vdots & \vdots & & \vdots \\ A_m & x_{m1} & x_{m2} & x_{m3} & \dots & x_{mn} \end{pmatrix}$$

Where A_i (i = 1,2,….,m) are possible alternative; X_j (j = 1,2,….,n) attribute with which alternative performance are measured; x_{ij} is the performance of A_i with respect to X_j.

5.2.1 Steps in TOPSIS method

The main procedure of TOPSIS method for selection of the best alternative from among those available is described below:

Step 1: Calculate the normalized decision matrix, $R = [r_{ij}]_{m\times n}$

$$r_{ij} = \frac{x_{ij}}{\sqrt{\sum_{i=1}^{m} x_{ij}^2}}, \ i=1,2,\ldots\ldots m;\ j=1,2\ldots\ldots n;$$

Step 2: Calculation of weighted normalized decision matrix,

$$V = [v_{ij}]_{m\times n}$$

$$v_{ij} = w_j \times r_{ij}, \ i=1, 2\ldots m;\ j = 1, 2\ldots n;$$

Where w_j is the weight of the j^{th} attribute and

$$\sum_{j=1}^{n} w_j = 1$$

The weights of the attributes can be calculated by standard deviation method

$$w_j = \frac{\sigma_j}{\sum_{k=1}^{n} \sigma_k}$$

Step 3: Determination of the ideal and negative ideal solution

(a) For Ideal solution:

$$A^+ = \{(\max v_{ij} \mid j\in J), (\min v_{ij} \mid j\in J') \mid i = 1,2,\ldots,m \}$$

$$= \{ V_1^+, V_2^+, V_3^+, \ldots\ldots\ldots\ldots\ldots\ldots, V_j^+, \ldots\ldots\ldots\ldots, V_n^+ \},$$

(b) For Negative Ideal solution:

$$A^- = \{(\min v_{ij} \mid j \in J), (\max v_{ij} \mid j \in J') \mid i = 1,2,\ldots,m \}$$

$$= \{ V_1^-, V_2^-, V_3^- \ldots V_j^- \ldots V_n^- \},$$

Where J = { j = 1,2,…….,n | j associated with beneficial criteria};

J'= { j = 1,2,…….,n | j associated with non-beneficial criteria}.

Step 4: Calculation of separation measure.

The separation of each alternative from the ideal solution is given as

$$S_i^+ = \sqrt{\sum_{j=1}^{n}\left(v_{ij} - V_j^+\right)^2}\ {}^2, i = 1,2,\ldots,m;$$

The separation of each alternative from the negative-ideal solution is given as

$$S_i^- = \sqrt{\sum_{j=1}^{n}\left(v_{ij} - V_j^-\right)^2}\ {}^2, i = 1,2,\ldots,m;$$

Step 5: Calculation of relative closeness of a perticular alternative to ideal solution can be expressed as:

$$C_i^+ = \frac{S_i^-}{S_i^+ + S_i^-}\ i = 1,2,\ldots,m;$$

Step 6: Ranking of the preference order is to be carried out. The value of C_i^+ indicate the most prefered and least prefered feasible solution. C_i^+ may also called the overall or composite perfermance score of alternative A_i.

5.3 RESULT AND DISCUSSION

In the present optimization closeness co-efficient calculated shown in Table 5.2. Taguchi applied on closeness co-efficient to get the optimal setting shown in Fig 5.1. Taguchi Orthogonal Array Design L16 (4**3) Factors: 3, Runs: 16.

Table5.2 Closness co-efficent and predictted values

Sl.no	d(mm)	f(mm/rev)	S(m/min)	S_i^-	S_i^+	c+	SNRA1	PSNRA1
1	0.10	0.04	57	0.621497	0.179617	0.22421	-12.987	26.0459
2	0.10	0.05	74	0.034833	0.956553	0.96486	-0.311	
3	0.10	0.06	96	0.10275	0.762361	0.88123	-1.098	
4	0.10	0.07	125	5.25e-13	1.347401	1.00000	0.000	
5	0.15	0.04	74	0.522721	0.371305	0.41532	-7.632	
6	0.15	0.05	57	0.687689	0.170911	0.19906	-14.020	
7	0.15	0.06	125	0.573695	0.287358	0.33373	-9.532	
8	0.15	0.07	96	0.798828	0.113247	0.12416	-18.120	
9	0.20	0.04	96	0.504222	0.297125	0.37078	-8.618	
10	0.20	0.05	125	0.653638	0.283729	0.30269	-10.380	
11	0.20	0.06	57	0.426267	0.632675	0.59746	-4.474	
12	0.20	0.07	74	1.347397	3.39e-12	0.00000	-231.991	
13	0.25	0.04	125	0.592814	0.185488	0.23832	-12.457	
14	0.25	0.05	96	0.4395571	0.840244	0.65654	-3.655	
15	0.25	0.06	74	0.754705	0.129718	0.14667	-16.673	
16	0.25	0.07	57	0.635468	0.221648	0.25860	-11.748	

The predicted value we get 26.0459, which is higher than calculated S-N ratio shown in above table.

5.3.1 Taguchi analysis

Response Table for Signal to Noise Ratios (Larger is better) shown in bellow table.

Table5.3 Response Table for Signal to Noise Ratios

Level1	d	f	S
1	-3.599	-10.423	-10.807
2	-12.326	-7.092	-64.152
3	-63.866	-7.944	-7.873
4	-11.133	-65.465	-8.092
Delta	60.267	58.373	56.279
Rank	1	2	3

5.3.2 Analysis on responses

In this present optimization, Main effect plot can be generated by using Taguchi technique and that plot can shows the optimal setting of the experiment shown in Fig 5.1.

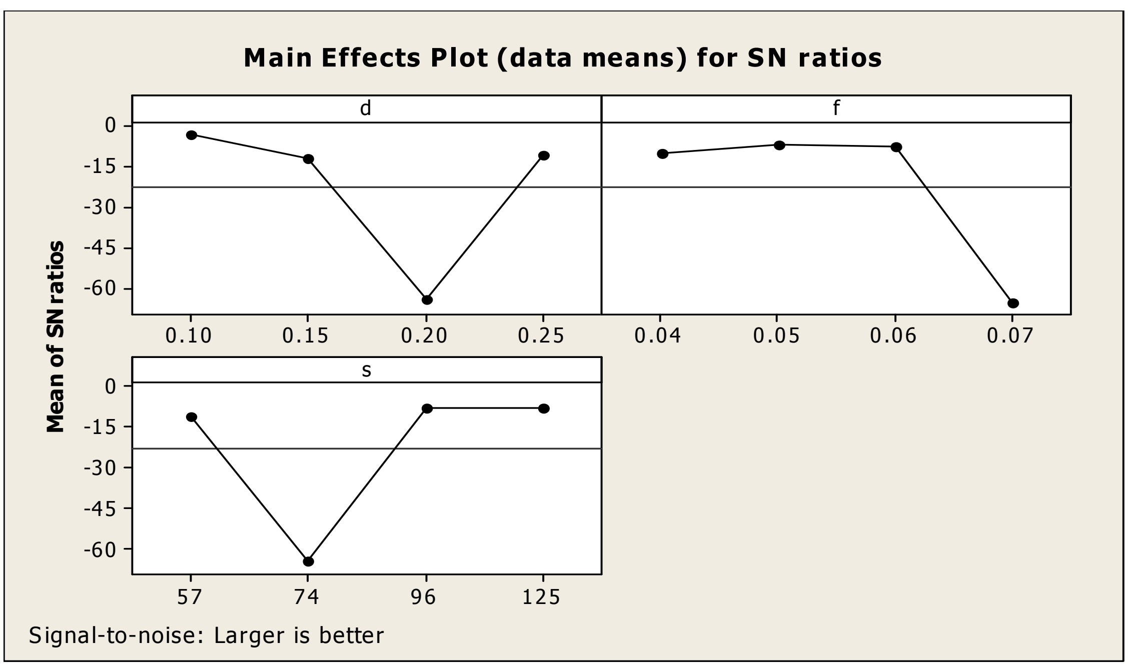

Figure 5.1 main effect plots

In the main effect plot larger is the better criteria is taken, than the optimum Factor levels for predictions d-0.1, f-0.06, S-96. In the 16 experiments, the optimum point is 3rd experiment wish is shown in table 5.2. The optimal point have in the experimental design so, no need to take the conformation test.

5.4 Summary

The results obtain from the experiment are compared with the predicted value calculated from the table.5.2. It can be seen that the regression model is reasonably better fitted with observed value.

Calculate the closeness co-efficient and applied the Taguchi to get the optimal setting based on main effect plot. The predicted value is higher than the calculated S-N ratio. So, the optimization is done.

Experiments were conducted according to Taguchi method by using the machining set up and the designed. The control parameters like depth of cut (d), feed (f), speed (S) varied to conduct 16 different experiments and the Surface roughness of the work piece and cutting forces were taken for calculation TOPSIS with Taguchi.

Chapter 6

6. CONCLUSIONS AND SCOPE FOR FURTHER WORK

6.1 CONCLUSION

In this present work the effect of cutting parameters (cutting speed, feed and depth of cut) on UAT and CT, cutting force and surface roughness measures on stainless steel has been investigated. The results have been compared with Ultrasonic assisted turning and conventional turning process. The influencing parameters of the horn design have also been investigated. The following conclusions could be drawn from this investigation:

- ✓ Measuring the surface roughness in Ultrasonic assisted turning as well as conventional turning on the work-piece. UAT improved the surface roughness by 12.0–45.0% compare with conventional turning. It proves that UAT can obtain smoother surface.
- ✓ FEA Analysis has been done to calculate the natural frequency of UVT. During the analysis of frequency response characteristics it is found out, that dominant peaks correspond the respective modes. Dominant peaks are in longitudinal direction at approximately 19.6 kHz excitation frequency. According to modal analysis the 2^{nd} mode is at excitation frequency 23.3 kHz. Here the cutting tool is vibrating in longitudinal direction.
- ✓ Compare forces on the work-piece both CT and UAT, The test results shows that the cutting force for the UAT method decreases by 20.0–33.0 % in UAT.
- ✓ The present study develops roughness and cutting force models for three different cutting parameters using new technique TOPSIS with Taguchi method. It is found that all the three cutting parameters (spindle speed, depth of cut and feed rate) and their interactions

have significant effect on roughness parameters considered in the present study though the influences may vary with the nature of work-piece material. Optimum machining parameter combinations for different roughness parameters are also tested through confirmation experiments that show fairly good agreement with prediction of TOPSIS with Taguchi method.

- ✓ To conclude, the UAT method has been found to be a suitable technique to achieve high-quality finish surfaces and lower cutting force requirement not only for hard material but also for general purpose engineering material, like Stainless steel (SS 304).

6.2 Scope for Further work

- More study is essential to know the effect of vibration parameters (amplitude, frequency, direction of vibration) on cutting performance in UAT.
- Also further analysis is required to find out the tool life, residual stress and temperature rise in UAT method.
- Further investigation is necessary to assess the impact of cutting tool edge condition, effect of rake angle and effect of the process on various materials.
- It is being suggested to make use of various cutting tools and various types of work-piece materials has to be to use in experimental procedure.
- Develop the coolant, to cool the Ultrasonic vibratory tool.
- Take the safety precautions while doing the experiment.

REFRENCES

[1] Shamato E.C. X. Ma and T. Morowaki, Ultraprecision ductile cutting of glass by applying ultrasonic elliptical vibration cutting, Precision Engineering Nanotechnology, 1, 1999, pp 408-411.

[2] Markov, A. I, Ultrasonic machining of intractable materials.1996.Lomdon: Iliffe Books Ltd.

[3] Kumabe, Journal of Vibratory cutting, 1979: Dzikke Sjuppan, Tokyo (in Japanese)

[4] Devin j., Ultrasonically assisted metal removal, SAMPLE Quarterly, 10, 1979, pp 485-496.

[5] Kremer D., Ultrasonically assisted machining, Mech. Ind. Mater. 48(1), 1995, pp.15-21.

[6] Astashev V.K, Effect of ultrasonic vibrations of a single point tool on the process of cutting, Journal of Machining. Manufacturing. Reliability, 5 (3), 1992, pp 65–70.

[7] Morowaki t., E. Shamoto and K. Inoue, Ultraprecision ductile cutting of glass by applying ultrasonic vibration, CIRP Annals, 1992, 41(1), pp 559-562.

[8] Astashev V. K., and Babitsky V. I., Ultrasonic cutting as a nonlinear (vibro-impact) process, Ultrasonic's, 36, 1998, pp 89-96.

[9] V.I. Babitsky, A. N. Kalashnikov, and A. Meadows, Ultrasonically assisted turning of aviation materials, Journal of Materials Processing Technology, 132, 2003, pp 157-167.

[10] Masahiko Jin, Masao Murakawa, Development of a Practical Ultrasonic Vibration Tool System. Journal of Materials Processing Technology, 113, 2001, pp 342-347

[11] constantin radu, catalin gheorghe amza. Research Regarding the Finite Element Modeling Of an Ultrasonic Horn Used In A Cutting Process, Materials Technology and Welding Department University Politehnica of Bucharest.

[12] Gheorghe AMZA, Doru Păuşan, Victor Popovici· Modeling using the finite element method of an ultrasonic stack used for ultrasonic spot welding. University Politehnica, Bucharest, 2007.

[13] Ainhoa Celaya, Luis Norberto López de Lacalle, Francisco Javier Campa and Aitzol Lamikiz. Ultrasonic Assisted Turning of mild steels, 2010. Faculty of Engineering, Department of Mechanical Engineering, University of the Basque Country, c/Alameda de Urquijo s/n, 48013 Bilbao, Spain.

[14] K. Liu, X.P. Li, and M. Rahman, Characteristics of ultrasonic vibration-assisted ductile mode cutting of tungsten carbide. The International Journal of Advanced Manufacturing Technology, 35, Nov. 2008, pp 833-841.

[15] J. Chen, G. Tian, Y. Chi, M. Liu, D. Shan, and Y. Liu, Surface Roughness and Microstructure in Ultrasonically Assisted Turning of W-Fe-Ni Alloy. Journal of Materials Processing Technology, 199, 2008, pp 441-444.

[16] C.Hsu, Y.Lin, W. Lee, and S. Lo, Machining characteristics of Inconel 718 using ultrasonic and high temperature-aided cutting, Journal of Materials Processing Technology, 198, Mar. 2008, pp 359-365.

[17] S. Amini, H. Soleimanimehr, M.J. Nateg, A. Abudolla, M.H. Sadegh, FEM analysis of ultrasonic-vibration-assisted turning and the vibratory tool, 2008. Tarbiat Modares University, Faculty of Engineering, Mech. Eng. Department, Tehran, Iran. Amir Kabir University of Technology, Mech. Eng. Department, Tehran, Iran.

[18] B.C.Behera, S.K.Sahoo, L.N. Patra, M.P.Rout, K.K.Kanaujia, 2011. Finite Element Analysis of Ultrasonic Stepped Horn, National Institute of Technology, Rourkela – 769 008, Orissa, India.

[19] Wu.Y., and Fan, Y., Develop an ultrasonic elliptical vibration shoe center less technique. Journal of Materials Processing Technology, 155-156, 2004, pp 1780-1787.

[20] B.C.Behera, S.K.Sahoo, K.P.Maity, Development and Experimental Study of Machining Parameters in Ultrasonic Vibration-assisted Turning. M.Tech thesis 2010-2011.

[21] Montgomery, D.C., & Myers, R.H. (2002). Response surface methodology, Wiley series in probability & statistics, 2nd edition. pp 1-5.

[22] S.K.Dewangan and C.K. Biswas (2010). Experimental Investigation of Machining Parameters for EDM Using U-shaped Electrode of AISI P20 Tool Steel. M.Tech thesis 2009-2011.

[23] Lee-ing Tong and Chao-Ton Su (1997). Multi-objective optimization of high-speed electrical discharge machining process using a Taguchi fuzzy-based approach. Materials and Design, 28, pp1159–1168.

[24] Hwang and Yoon (1981). Evolutionary programming method for modeling the EDM parameters for roughnesses, Journal of Materials Processing Technology, 200, pp 347–355.

[25] Lan, T.S. (2009). Taguchi optimization of multi-objective CNC machining using TOPSIS, Information Technology Journal 8(6), pp917-922.

[26] Mitrofanov,A., Babitsky,V. & Silberschmidt,V., Thermo mechanical finite element simulations of ultrasonically assisted turning. Computational Materials Science, 32(3-4), 2005, pp 463-471.

[27] Mitrofanov, A., Ahmed, N., Babitsky, V. & Silberschmidt, V., Effect of lubrication and cutting parameters on ultrasonically assisted turning of Inconel718. Journal of Materials Processing Technology, 162-163, 2005, pp 649-654.

[28] Ahmed, N., Mitrofanov,A., Babitsky,V.& Silberschmidt,V , Analysis of material response to ultrasonic vibration loading in turning Inconel718. Materials Science and Engineering, 424(1-2), 2006. pp 318-325.

[29] Klocke F, Kratz H. Advanced tool-edge geometry for high-precision hard turning. CIRP ANN, 54(1), 2005; pp 47–50.

[30] Adachi, K., Arai, N., Harada, S., Okita, K., and Wakisaka, S., A study on burr in low frequency vibratory drilling of aluminum. Surface Metrology, Measurement Science and Technology, 8, 1997, pp. 955-972.

[31] Wu.Y., and Fan, Y., Develop an ultrasonic elliptical vibration shoe center less technique. *Journal of Materials Processing Technology*, 155-156, 2004, pp 1780-1787.

[32] Roark R .J and Young W.C., Formulas for stress and strain, 5th ed., McGraw-Hill, NY, 1975.

[33] ANSYS® 12.0 User guides.

[34]. Myers R. and Montgomery D., Response Surface Methodology, Process and Product Optimization Using Designed Experiments. Wiley, New York. 1995.

[35]Minitab®14.0 User guides.